DESIGN, CONSTRUCTION AND TESTING OF A ZEOLITE-WATER SOLAR ADSORPTION REFRIGERATOR

BY

AMBER ITYONA

DEPARTMENT OF MECHANICAL ENGINEERING
AHMADU BELLO UNIVERSITY, ZARIA
NIGERIA

JUNE, 2008

DESIGN CONSTRUCTION AND TESTING OF A ZEOLITE-WATER SOLAR ADSORPTION REFRIGERATOR

BY

AMBER ITYONA B.ENG (ABU 2003)
MSC/ENG/51362/05-06

A DISSERTATION SUBMITTED TO THE POSTGRADUATE SCHOOL,
AHMADU BELLO UNIVERSITY, ZARIA
NIGERIA

IN PARTIAL FULFILLMENT FOR THE AWARD OF MASTER OF SCIENCE IN MECHANICAL ENGINEERING

DEPARTMENT OF MECHANICAL ENGINEERING
AHMADU BELLO UNIVERSITY, ZARIA
NIGERIA

JUNE, 2008

DECLARATION

I declare that the work in the dissertation entitled 'Design, construction and testing of a Zeolite-water solar adsorption refrigerator' has been performed by me in the Department of Mechanical Engineering under the supervision of Prof C.O Folayan. The information derived from the literature has been duly acknowledged in the text and list of references provided. No part of this dissertation was previously presented for another degree or diploma at any University.

CERTIFICATION

This dissertation entitled "DESIGN CONSTRUCTION AND TESTING OF A ZEOLITE-WATER SOLAR ADSORPTION REFRIGERATOR" by Amber Ityona meets the regulations governing the award of the degree of Masters in Science in Mechanical Engineering Ahmadu Bello University, Zaria, and is approved for its contribution to knowledge and literary presentation

_____ Date _____

Prof C.O Folayan
Chairman, supervisory committee

_____ Date _____

Dr. D.S Yawas
Member, supervisory committee

_____ Date _____

Prof C.O Folayan
Head of Department

_____ Date _____

Prof S.A Nkom
Dean, PostGraduate School

ACKNOWLEDGEMENT

First, I thank God almighty for the gift of life, provision and protection throughout the course of this project.

A special thanks goes to my supervisor Professor C.O Folayan for his continuous support in the MS.c program ; I highly acknowledge his patience , tolerance , careful guidance, thorough supervision and vetting of the manuscript.

I also acknowledge the assistance of the chair Chemical Engineering Dept, petroleum technology development fund (PTDF) particularly Engr.A.A Attah and Prof S.S Adefila for their constructive criticism, encouragement, useful exchange of information and material assistance in making this project a reality.

Lastly I acknowledge the entire staff of the Mechanical Engineering Department for their contributions and assistance over the period I undertook this work.

ABSTRACT

A simple solar energy powered intermittent adsorption refrigeration system was designed,

fabricated and tested. The system uses a Zeolite as the adsorber and water as the working fluid. The heat source is a parabolic trough concentrator which is to collect and concentrate solar thermal energy onto a black body coated copper absorber. The generator drives the refrigerant around the system through a condenser and an evaporator to complete the refrigeration cycle. Two set of test were carried out and different times of the year, one in January 2008 a month with the lowest solar irradiation and the second set in May 2008. The system was evaluated by leaving it outside under solar radiation and monitoring temperatures at various points on the the generator, condenser and the evaporator through the use of thermocouple sensors. The first test carried out revealed that the average highest and lowest temperatures on the solar collector were 57.2^{o}C and 11.5°C respectively. The average lowest refrigeration temperature was 18°C. No cooling effect was actually produced due to the period testing was carried out and imperfection in the fabrication process. The Zeolite was produced in locally with a pore size of 4 $^{\cdot}$ and a regenerative temperature of 250^{o}C. The second test carried out in May 2008 produced a cooling effect by making small changes on the system. An evaporator temperature of 9^{o}C was attained which linearly increased to a maximum of 28^{o}C as the day advanced. Maximum absorber temperature of 64^{o}C was attained over the test period.TGA and DTA confirmed the regenerative temperature to be at 200^{o}C and to be thermally stable at 600^{o}C.

TABLE OF CONTENTS

Cover page i
Declaration iii
Certification iv
Acknowledgement v
Abstract vi

CHAPTER ONE

1.0 Introduction 1
1.1 History of refrigeration 2
1.1.1 The industry today 4
1.2 Solar cooling paths 5
1.3 Refrigeration system 7
1.3.1 Vapor compression system 7
1.3.2 Absorption refrigerator 8
1.3.3 Adsorption refrigeration cycle 9
1.3.4 Gas expansion refrigeration 11
1.3.5 Thermoelectric refrigeration 12
1.3.6 Evaporative cooling 12
1.4 Statement of the problem 14
1.5 Objectives 15
1.6 Justifications 15

CHAPTER TWO

2.0 Literature review 18

2.1 Review of past works in the area 18

2.2 Characteristics of the adsorbent- adsorbate pair 21

2.3 Zeolite 22

2.3.1 Commercial and domestic uses 22

CHAPTER THREE

3.0 Design theory 24

3.1 Adsorption cycles for solar cooling 26

3.2 Design of the cooling system 29

3.3. Heat load calculation 30

3.4 Product load 32

3.5.1 Usage load 32

3.5.2 Design of the evaporator 32

3.5.3 Design of the condenser 34

3.5.4 Collector design 36

3.5.5 Design of the parabolic trough 36

3.5.6 Design requirements for concentrators 36

3.5.7 Collector sizing 37

3.8.4 Receiver tube diameter 37

3.9 Energy balance for the parabolic trough concentrator 38

3.9.1 One dimensional energy balance model 39

3.9.2 Convection Heat Transfer between HTF and the Absorber 42

3.9.3 Conduction heat transfer through the absorber wall 43

3.9.4 Convective heat transfer 44

3.9.5 Radiation heat transfer 44

3.9.8 Optical properties 44

3.9.7 Solar irradiation absorption in the absorber

3.9.8 No glass envelope case 45

3.10 Design calculations 47

CHAPTER FOUR

4.0 Introduction 60

4.1 Construction 60

4.2 Methodology 61

4.3 Production of Zeolite A 61

4.4 Collector structure fabrication 62

4.5 Construction processes 64

4.6 Assembly 67

4.7 Testing 69

4.8 Results 71

4.9 Discussions 77

4.10 Cost of production of the refrigerator 79

CHAPTER FIVE

5.0 Summary 84

5.1 Conclusion 85

5.2 Recommendations 86

LIST OF FIGURES

Fig 1.1 The possible paths from solar energy to cooling services 6

Fig 1.2 Main components of a vapour-compression refrigerator, and *T-s* and *p-h* diagrams of the processes. 8

Fig. 1.3. Layout of an absorption refrigeration machine, showing inputs and outputs 9

Fig 1.4 The adsorption cycle 10

Fig. 1.5. Gas expansion refrigeration cycle 11

Fig. 1.6 Sketch of a thermo-electric-cooler (TEC) with three thermo-elements 12

Fig 3.1a Adsorption phase of a Zeolite system 26

Fig 3.1 b Desorption phase of a Zeolite system 27

Fig 3.2 - Schematic diagram of the simple adsorption refrigerator 27

Fig 3.3: An ideal adsorption cooling cycle in the Duhring diagram 28

Fig 3.4: Cooling Box 30

Fig. 3.5: Cross – section of cooling box 31

Fig 3.6: Thermal Losses Proportional to Receiver Tube Diameter 38

Fig 3.7:(a) Energy balance (with glass envelope) 41

Fig. 3.8 (b): Energy balance without glass envelope 41

Fig. 3.9: Thermal resistance model with glass envelope 41

Fig. 3.10: Thermal resistant model without glass envelope 42

Fig4.1 Produced Zeolite 62

Fig 4.2 Showing the parabolic trough concentrator 68

Fig 4.2 Zeolite-water solar adsorption refrigerator 69

Fig 4.3 Testing set-up 70

Fig 4.2 Showing the parabolic trough concentrator 76

Fig 4.4 Desorption curves for Zeolite A 78

Fig 4.5 Temperature profile for 6th may 2008 76

Fig 4.6 Temperature profile for 7th may 2008 76

Fig 4.7 Temperature profile for 8th may 2008 77

Fig 4.8 Desorption curves for Zeolite A 81

LIST OF TABLES

Table 1.0 Historical development in refrigeration and air conditioning 1

Table 4.1 Readings 14th Jan2008 73

Table4.2 Readings 15th Jan2008 73

Table 4.3 Readings 16th Jan2008 74

Table 4.4 Readings 17th Jan 2008 74

Table 4.5: Readings 18th Jan 2008 75

Table 4.6 Readings 6th May2008 74

Table 4.7 Readings 7th May 2008 74

Table 4.8: Readings 8th May 2008 75

Table 4.9 Some determined properties of the produced Zeolite A 76

Table 4.10: Cost of Zeolite production 80

Table 4.11: Solar refrigerators materials and cost 81

NOMENCLATURE

α = adsorptivity [m^2/s]

α_{abs} = absorptance of the absorber selective coating

α_{env} = absorptance of the glass envelope

A_{cs} = absorber pipe cross-sectional flow area [m^2]

$A_{cs,b}$ = minimum cross-section of receiver support bracket [m^2]

A_i = circumferential area of receiver segment "i" [m^2]

C.O.P= coefficient of performance

δ = molecular diameter of annulus gas [cm]

c = specific heat [J/kg-K]

σ = Stefan-Boltzmann constant [$W/m^2\text{-}K^4$]

δ = declination [^{o}]

D_2 = inside diameter of absorber pipe [m]

D_3 = outside diameter of absorber pipe [m]

D_4 = inside diameter of glass envelope [m]

D_5 = outside diameter of glass envelope [m]

ε = equivalent surface roughness [m]

$\varepsilon'_{\#}$ = optical efficiency terms

ε_3 = emissivity of absorber selective coating

ε_4 = emissivity of inner surface of glass envelope

ε_5 = emissivity of outer surface of glass envelope

f = Darcy friction factor

f_2 = friction factor for the inner surface of the absorber pipe

f_i= cooling coefficient

g = gravitational constant, 9.81 m/s^2

h_1 = convection heat transfer coefficient for the HTF at T_1 [W/m^2-K]

h_{34} = convection heat transfer coefficient of annulus gas at T_{34}[W/m^2-K]

h_{56} = convection heat transfer coefficient of air at T_{56} [W/m^2-K]

$h_{i,}$ = enthalpy at inlet of receiver segment "i" [J/kg]

h_o = enthalpy at outlet of receiver segment "i" [J/kg]

HCE = Heat collector element

HTF = Heat transfer fluid

K = incident angle modifier

k = thermal conductance [W/m-K]

k_1 = thermal conductance of HTF at T_1 [W/m-K]

k_{23} = thermal conductance of absorber wall at T_{23} [W/m-K]

k_{34} = thermal conductance of annulus gas at T_{34} [W/m-K]

k_{56} = thermal conductance of air at T_{56} [W/m-K]

k_b = conduction heat transfer coefficient of air evaluated at the average receiver support bracket film temperature for receiver segment "i" [W/m-K]

k_{std} = thermal conductance of annulus gas at standard temperature and pressure [W/m-K]

$\dot{}$ = mass flow rate [kg/s]

n_i = number of receiver support brackets on receiver segment "i"

γ = ratio of specific heats

η_{abs} = effective optical efficiency at the absorber

η_{env} = effective optical efficiency at the glass envelope

Nu_{D2} = Nusselt number of HTF based on D_2

Nu_{D5} = Nusselt number of air based on D_5

ρ = density [Kg/m^3]

π = ratio of the circumference to diameter of a circle, 3.14159

P_a = annulus gas pressure [mmHg]

P_b = exterior perimeter of receiver support bracket [m]

$P_{inlet,i}$ = HTF pressure at inlet of receiver segment "i" [^oC]

$P_{outlet,i}$ = HTF pressure at outlet of receiver segment "i" [^oC]

Pr_1 = Prandtl number of HTF evaluated at T_1

Pr_2 = Prandtl number of HTF evaluated at T_2

Pr_{34} = Prandtl number of annulus gas at T_{34}

Pr_5 = Prandtl number of air at T_5

Pr_{56} = Prandtl number for air at T_{56}

Pr_6 = Prandtl number of air at T_6

P_v = vapor pressure [kPa]

P_w = absorber pipe inner wetted surface perimeter [m]

θ = solar incident angle from the normal to the projected collector area [degrees]

$q_{12\ conv}$ = convection heat transfer rate between the heat transfer fluid and inside wall of the absorber pipe per unit receiver length [W/m]

$q_{23\ cond}$= conduction heat transfer rate through the absorber pipe wall per unit receiver length [W/m]

$\dot{q}'_{3SolAbs}$= solar irradiation absorption rate into the absorber pipe per unit receiverlength [W/m]

$\dot{q}'_{3\ SolAbs\ i}$ = incident solar irradiation absorption rate into the absorber pipe of receiver segment "i" per unit segment length [W/m]

$\dot{q}'_{34\ conv}$ = convection heat transfer rate between the outer surface of the absorber pipe to the inner surface of the glass envelope per unit receiver length [W/m]

$q'_{34\ conv\ i}$ = convection heat transfer rate for receiver segment "i" between the outer surface of the absorber pipe to the inner surface of the glass envelope per receiver segment length [W/m]

$q'_{34\ rad}$ = radiation heat transfer rate between the outer surface of the absorber pipe to the inner surface of the glass envelope per unit receiver length [W/m]

$q'_{34\ rad\ i}$ = radiation heat transfer rate for receiver segment "i" between the outer surface of the absorber pipe to the inner surface of the glass envelope per receiver segment length [W/m]

$\dot{q}_{36\ conv}$ = convection heat transfer rate between the outer surface of the absorber pipe to the atmosphere per unit receiver length [W/m]

$\dot{q}_{36\ conv\ i}$ = convection heat transfer rate between the outer surface of the absorber pipe to the atmosphere per unit receiver segment length for receiver segment "i" [W/m]

$\dot{q}'_{57\ rad}$ = radiation heat transfer rate between the outer surface of the glass envelope to the sky per unit receiver length [W/m]

$q'_{37\ rad\ i}$ = radiation heat transfer rate between the outer surface of the absorber pipe to the sky per unit receiver segment length for receiver segment "i" [W/m]

$\dot{q}'_{45cond}$ = conduction heat transfer rate through the glass envelope per unit receiver length [W/m]

$\dot{q}'_{5SolAbs}$ = solar irradiation absorption rate into the absorber pipe per unit receiver length per unit receiver length [W/m]

$\dot{q}'_{5SolAbs\ i}$ = incident solar irradiation absorption rate into the glass envelope of receiver segment "i" per unit segment length [W/m]

$\dot{q}'_{56conv}$ = convection heat transfer rate between the outer surface of the glass envelope to the atmosphere per unit receiver length [W/m]

$\dot{q}'_{37rad}$ = radiation heat transfer rate between the outer surface of the absorber pipe to the sky per unit receiver length [W/m]

$\dot{q}'_{cond\ bracket\ i}$ = conductive heat loss through each receiver support bracket on receiver segment "i" [W]

$q'_{cond\ bracket\ total\ i}$ = total conductive heat losses through all receiver support brackets on receiver segment "i" [W]

$q'_{HeatLoss}$ = total heat loss rate from the heat collecting element to the surroundings [W/m]

$\dot{q}'_{HeatLoss\ i}$ = heat loss rate per unit circumferential area to the atmosphere from receiver segment "i" (excluding bracket losses) [W/m^2]

$q'_{HeatLoss\ total\ i}$ = total heat loss rate per unit circumferential area from receiver segment "i" [W/m^2]

q'_{i} = net heat flux per unit circumferential area of receiver segment "i" [W/m^2]

q'_{si} = solar irradiance per receiver unit length [W/m]

$\dot{q}''_{SolarAbs\ i}$ = incident solar irradiation absorption rate per unit circumferential area of receiver segment "i" [W/m^2]

$q_{cond,bracket}$ = total conductive losses through receiver support brackets [W]

$q_{HeatLoss}$ = heat loss per receiver length [W/m]

Ra_{D3} = Rayleigh number of annulus gas based on D_3

Ra_{D5} = Rayleigh number of air based on D_5

Re_{D2} = Reynolds number of HTF based on D_2

$Re_{D2,ave,i}$ = Reynolds number based on D_2 and evaluated at the average HTF bulk temperature of receiver segment "i"

Re_{D5} = Reynolds number of air based on D_5

T = temperature [^{o}C]

T_a = ambient temperature [^{o}C]

T_1 = mean (bulk) temperature of the HTF [^{o}C]

T_2 = absorber pipe inner surface temperature [^{o}C]

T_{23} = average absorber wall temperature, (T2 + T3)/2 [^{o}C]

T_3 = absorber pipe outer surface temperature [^{o}C]

T_{34} = average temperature of annulus gas, (T3+T4)/2 [^{o}C]

T_4 = glass envelope inner surface temperature [^{o}C]

T_5 = glass envelope outer surface temperature [^{o}C]

T_{56} = average temperature of air, (T_5 + T_6)/2 [^{o}C]

T_6 = atmosphere temperature [^{o}C]

T_7 = estimated effective sky temperature [^{o}C]

$T_{base,i}$ = temperature at base of receiver support bracket for receiver segment "i" [^{o}C]

$T_{inlet,i}$ = HTF temperature at inlet of receiver segment "i" [^{o}C]

$T_{outlet,i}$ = HTF temperature at outlet of receiver segment "i" [^{o}C]

τ_{env} = transmittance of the glass envelope

μ = dynamic viscosity [kg/m-s]

$\mu_{ave,i}$ = dynamic fluid viscosity of HTF at the average temperature of receiver segment "i" [Ns/m^2]

v_{56} = kinematic viscosity of air at T_{56} [m^2/s]

$v_{i,in}$ = bulk fluid velocity at inlet of receiver segment "i" [J/kg]

$v_{i,out}$ = bulk fluid velocity at outlet of receiver segment "i" [J/kg]

Δh_i = change in enthalpy through receiver segment "i" ($h_{inlet,i} - h_{outlet,i}$) [J/kg]

$\Delta L_{aperture}$ = receiver segment length [m]

ΔP_i = change in HTF pressure through receiver segment "i" ($P_{inlet,i} - P_{outlet,i}$) [Pa]

ΔT_i = change in HTF temperature through receiver segment "i" ($T_{inlet,i} - T_{outlet,i}$) [K]

$\rho_{ave,i}$ = HTF density at average temperature of receiver segment "i" [kg/m^3]

CHAPTER ONE

4.0 INTRODUCTION

Refrigeration is a term used to describe a process which maintains a process space or material at a temperature less than the ambient temperature. To accomplish this, heat must be transferred from the materials to be cooled into a lower temperature substance referred to as a refrigerant. With advancement in science and technology, the role and function of refrigeration and its application have steadily become indispensable to the existence of the modern society.

The concept of using solar energy for powering a refrigerator appeared forty years ago with a prototype using a liquid sorption cycle, Sumathy (1999). The use of sorption processes to produce refrigeration has been extensively studied in the last twenty years as a technological alternative to vapour compression systems. Solar-powered refrigeration can also use solid sorption, with either a chemical reaction, or adsorption. Several theoretical and experimental studies demonstrated that sorption refrigeration systems especially those using solid-gas heat cycles are well adapted to simple technology applications. They can operate without moving parts and with low grade heat from different sources such as residual heat or solar energy. The main two technologies concerning the solid – gas sorption concept are the adsorption and the chemical reaction, including metal hydrides. The similarities and differences between these systems as well as the advantages and disadvantages of each one are extensively described by Meunier (1998)

Solar powered refrigeration and air conditioning have been very attractive during the last twenty years, since the availability of sunshine and the need for refrigeration both

reach maximum levels in the same season. One of the most effective forms of solar refrigeration is in the production of ice, as ice can accumulate much latent heat, thus the size of the ice-maker can be made small. Solid adsorption refrigeration makes use of the unique features of certain adsorbent-refrigerant pairs to complete refrigeration cycles for cooling or heat pump purposes. Zeolite and activated carbon were used as adsorbents in many systems. Based on his studies Ing. (2004) recommended that Solid adsorption pair of Zeolite and water is best to produce refrigerating effect while activated carbon and methanol can serve as a suitable pair for a solar powered, solid-adsorption ice-maker.

.

1.1 HISTORY OF REFRIGERATION

A comparative summary of the historical developments in refrigeration and air conditioning is presented in Table 1.

Table 1. Historical development in refrigeration and air conditioning. Jordan (1962)

Date	Refrigeration	Air conditioning
15th c. B.C.	First mention of making ice, in ancient Egypt, by night-cooling, for refreshment and fever treatment.	Evaporative cooling used to cool air in dry climate by water splashing.
2nd. A.D.	Galen proposes four degrees of coldness (and four degrees of heating).	
1700	First artificial ice production, by aspirating ether vapours, for medical purpose.	
1800	Natural ice regional and world-wide markets expand.	J. Gorrie in Florida made a

	Ferdinand Carré invented in 1846 the ammonia absorption cycle.	hospital-ward refrigerated by blowing air with a fan over ice, to prevent diseases.
1865	First commercial ice-makers, using Carré's ammonia absorption plants.	
1873	First commercial refrigerator, by von Linde, using an ammonia vapour compressor. The first closed-loop vapour compression refrigerator was patented in London by J. Perkins.	Linde also built the first domestic air conditioning (for an Indian Rajah).
1880	First frozen-meat ocean transport, using air compression and expansion.	
1900	Development of large artificial ice-making firms, using ammonia compressor driven by a steam engine.	First refrigerated public building in 1901.
1911		Carrier, in an ASME meeting, presented the refrigerator-dehumidifier
1914	Kelvinator introduces the thermostatic valve.	
1918	Frigidaire (assoc. to GM) sells domestic units at $1000.	
1920s	GE develops the sealed compressor in 1928. Frigidaire units at $500 (still bulky: 170 kg). One million units sold, mostly using SO_2.	Carrier units in theatres and cinemas.
1925	Electrolux developed an absorption refrigerator	

	without moving parts (marketed in USA by Servel).	
1928	T. Midgely found a safe refrigerant, CCl_2F_2, commercially synthesised in 1929 by DuPont-GM from CCl_4 and HF, trade-named as Freon.	
1932		Small window units by GE.
1934	Door-shelves were proposed, but were discarded.	
1939	GE develops the two-doors combined frigo-freezer.	First car air conditioning unit.
1960	Domestic refrigerators popularise; replacing ice-chests.	Most American shopping centres and hotels conditioned.
1980	Self-defrosting units. Domestic units with ice-cube and chip-ice dispensers.	Domestic air conditioning popularised.

The history of refrigeration is nearly the same as the history of making ice, artificial ice, since the history of natural ice is another story: homo-sapiens era is the quaternary period in the history of Earth, the last 2 million years, and, although there have been little climatic changes during the last 10 000 years (Holocene), during the rest of the quaternary period (Pleistocene) major ice ages occurred, lasting some 100 000 years each (with intermediate warm periods of some 10 000 years), with polar ice caps extending to middle latitudes (although the average Earth surface temperature was just 9 ºC below the present 15 ºC). Jordan (1962):

1.1.1 The industrial applications

The expansion of the refrigeration industry over the years has been very great indeed, with exception of the radio industry, no other field had such a rapid acceptance and emerging impact upon our lives. Over the years new industrial applications have opened comparatively new fields in controlled temperature application, Application of refrigerator in the medical profession are increasing daily not only in the preservation of certain products, but also in the actual treatment of some physical ailments; also in the refrigerated food industry development are occurring so rapidly that it is difficult to keep abreast of them. Increased applications of domestic refrigerators have been supplemented by the use of low grade energy sources for domestic low temperature refrigerator.

These are few, but the wide spread application of refrigerator. Present day refrigeration requirements involve the entire comparative scale, almost down to absolute zero, with great consideration the challenges facing the energy sector of the economy.

1.2 SOLAR COOLING PATHS

Solar powered cooling systems can generally be classified into 3 main parts:-

i. Solar energy conversion equipment

ii. The refrigeration system

iii. Cooling loads

Solar driven refrigerator system can further be classified into two main groups as shown in fig 1.1 ,depending on the mode of energy supplied namely:-

a. Thermal/work driven systems:- solar thermal conversion to heat Adsorption.

- Chemical reaction
- Desiccant cooling cycle
- Ejector refrigeration cycle
- Rankine refrigeration cycle

b. Electrical (photovoltaic) driven systems – process to electricity

- Stirling refrigerator cycle
- Thermoelectric Peltier refrigerator cycle
- Vapour compressive refrigerator cycle

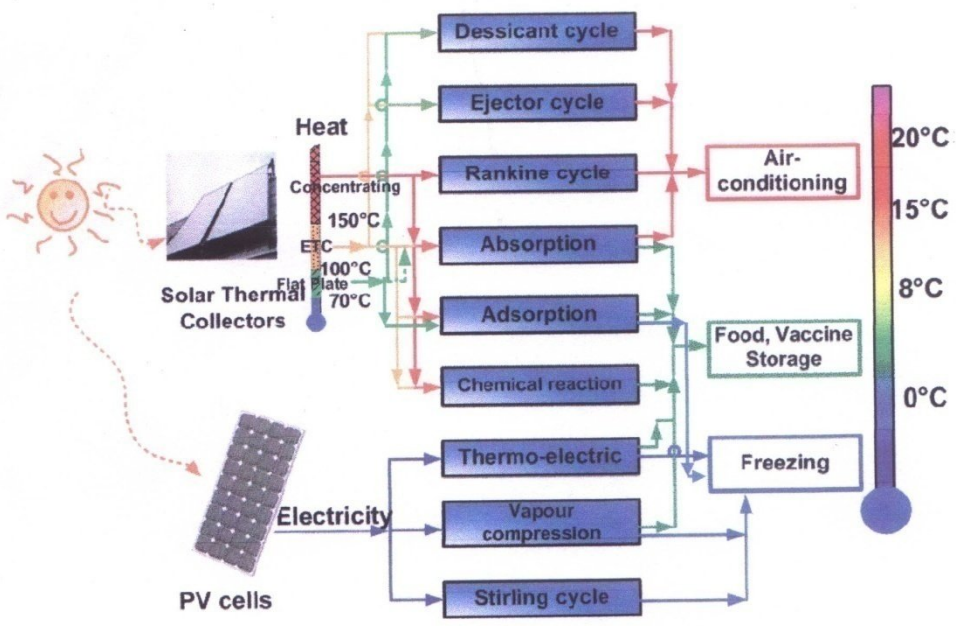


Fig 1.1 The possible paths from solar energy to cooling services

Each group can be classified according to the type of refrigerator cycle. The appropriate cycle in each application depends on cooling demand, power and the temperature levels of the refrigerated object and the environment.

1.3 REFRIGERATION SYSTEMS

Refrigerating effect is produced by the removal of heat from the substance to be cooled. This phenomenon takes place with the aid of a cooling medium to which the heat flows, to a lower temperature than the substance being refrigerated.

Before advent of modern refrigeration process, water was kept cool by storing it in earthen ware jugs so that the water could flow through the pores and evaporate.

Natural ice from lakes and rivers were often cut during the winter and stored in caves straw-lined pits and later in saw dust –insulated buildings. The early Romans carried packed trains of snow from the Alps to Rome for cooling the emperor's drinks. These methods are all natural ways of refrigeration.

Artificial Refrigeration is produced in many ways which include:-

- Vapour compression
- Absorption refrigeration
- Adsorption
- Thermoelectric
- Gas expansion refrigeration

1.3.2 Vapour compression system

A common and effective cold producing technology is based on the vacuum vaporization of volatile liquid. Compression is accomplished either mechanically or by absorption vapour compression refrigeration cycle based on a modified reverse Rankine cycle. Saturated or slightly saturated vapour is pumped by a compressor to a high pressure then cooled until the compressed gas condenses to a liquid and the saturated or slightly saturated cycle flashes to the low pressure vaporized through a valve. Jordan (1962)

Vapour compressor cycles usually work with single component refrigerant, but some times Mixtures are used. Fig 1.2 main components of a vapour compression system

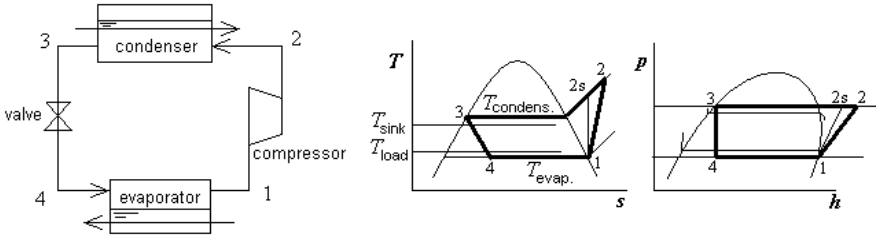


Fig 1.2 Main components of a vapour-compression refrigerator, and *T-s* and *p-h* diagrams

1.3.2 **Absorption refrigerator**

An absorption refrigeration machine corresponds to vapour-compression refrigerator in which the compressor is substituted by four elements: vapour absorber, based on another liquid, a pump for the liquid solution, a generator or boiler to release the vapour from solution and a valve to recycle the absorbent liquid. Its advantage is that the cycle requires less work to operate or none at all if the liquid is naturally pumped by gravity in a thermo-siphon, at the expense of an additional heat source required at the regenerator Jordan (1962).The basic scheme is presented in Fig. 1.3.

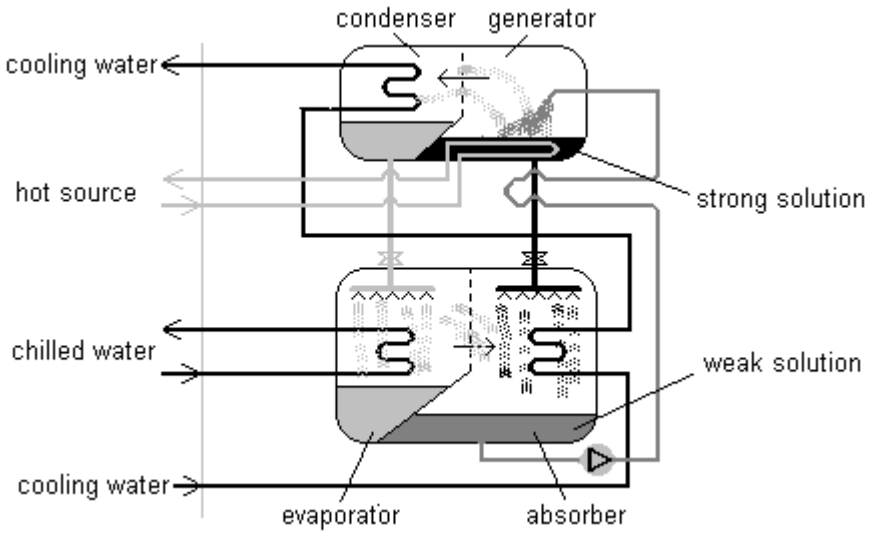


Fig. 1.3. Layout of an absorption refrigeration machine,

There are two working fluids of an absorption refrigerator. The refrigerant and the carrier (the auxiliary liquid) that absorbs the refrigerant and is pumped up to high pressure and release the refrigerant vapour at the generator. Ammonia has been traditionally used as refrigerant in both types of refrigeration.

1.3.3 Adsorption refrigeration cycle

An adsorption, also called a solid-sorption cycle, is a preferential partitioning of substances from a gaseous or liquid phase onto a surface of a solid substrate. This process involves the separation of a substance from one phase to accumulate or concentrate on a surface of another substance. An adsorbing phase is called an 'adsorbent'. Material, which is accumulated, concentrated or adsorbed in another surface, is called an 'adsorbate'. The sticking process should not change any macroscopic of the adsorbent except the changing in adsorbent's mass.

Both adsorption and absorption can be expressed in term of sorption process. The adsorption process is caused by the Van der Vaals force between adsorbates and atoms or molecules at the adsorbent surface. The adsorbent is characterised by the surface and porosity.

In the adsorption refrigeration cycle, refrigerant vapour is not to be compressed to a higher temperature and pressure by the compressor but it is adsorbed by a solid with a very high microscopic porosity. This process requires only thermal energy, no mechanical energy requirement. The principles of the adsorption process provide two main processes, adsorption or refrigeration and desorption or regeneration.

The refrigerant (water) is vaporised by the heat from cooling space and the generator (absorbent tank) is cooled by ambient air. The vapour from the cooling space is lead to the generator tank and absorbed by adsorbent (Zeolite). The rest of the water is cooled or frozen.

In the regeneration process, the Zeolite is heated at a high temperature until the water vapour in the Zeolite is desorbed out, goes back and condenses in the water tank, which is now acting as the condenser.

For an intermittent process, the desorption process can be operated during daytime by solar energy, and the adsorption or the refrigeration process can be operated during night-time. The solar energy can be integrated with a generator. The single adsorber is required for a basic cycle. The number of adsorbers can be increased to enhance the efficiency, which depends on the cycle. This process can also be adapted to the continuous process

The adsorption refrigeration cycle relies on the adsorption of a refrigeration gas into an adsorbent at low pressure and subsequently desorbed by heating. The adsorbent also acts as a "chemical compressor" driven by heat. In its simplest form an adsorption refrigerator consists of two linked vessels, one of which contains adsorbent and both of which contain refrigerant as shown in Figure 1.4 Critoph [1999].

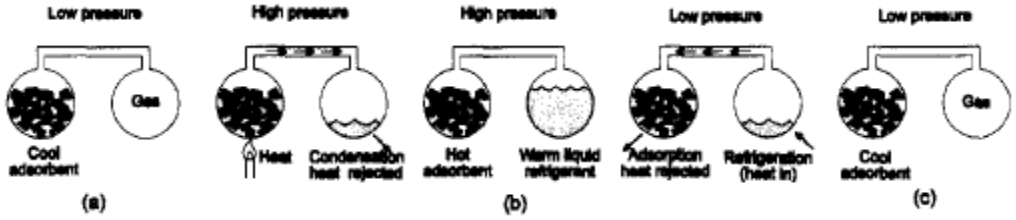


Fig 1.4 The adsorption cycle

In the first step, the whole system is at low pressure and contains refrigerant gas. The adsorbent contains a large quantity of gas. In the second step, the adsorbent is heated and rejects the gas which condenses in the second vessel. While it condenses, it rejects heat. During the third step, the whole system is at high pressure. In the fourth step the

gas evaporates and is readsorbed by the adsorbent. During this step, the gas takes heat for evaporation. In the final step, the system is at the same state than in the first step. This system produces cold during a half part of the cycle, to produce cold continuously; two such cycles must be worked out of phase. The adsorbent is made of activated carbon and the refrigerant gas is ammonia. For increase the performance of the system, two beds could be used.

1.3.4 Gas expansion refrigeration

An adiabatic expansion of a closed system always reduces its internal energy with a decrease in temperature i.e. a refrigeration effect proportional to the expansion (that is why gases are used instead of condensed matter). An adiabatic expansion in a work producing flow system always reduces the enthalpy with a decrease in temperature, but an adiabatic expansion in a liquid flow system, maintain the total enthalpy and may decrease or increase its temperature depending on the relative side of the inversion temperature.

Gas expansion cycles are only used in special applications as for cryogenic refrigeration and for special applications where compressed air is already available, as from gas turbine engines and in cabin –air conditioning on airplane. Gas expansion cycles basically corresponds to an inverted Brayton cycles. Small stirling cycle refrigerators have been developed using helium as a working fluid as illustrated in fig 1.5 below. Awoniyi (1980)

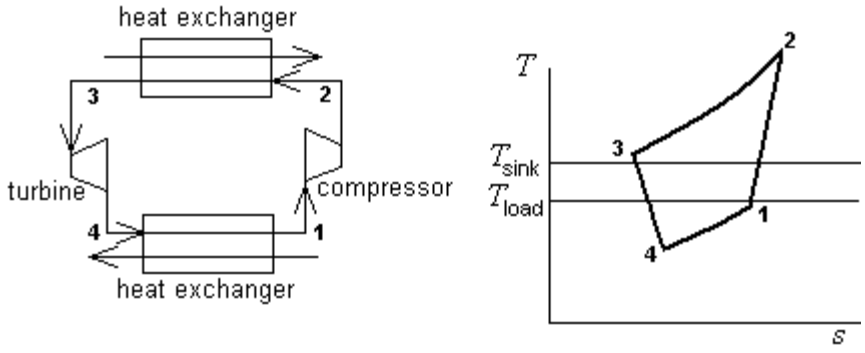


Fig. 1.5. Gas expansion refrigeration cycle

1.3.5 Thermoelectric refrigeration

Solid state electrically driven refrigerators (also called thermoelectric coolers TEC) are based on the Peltier effect when a direct current flows in a circuit formed by the dissimilar electrical conductors, some heat is absorbed at one junction and some more heat is released at the other junction, reversing the effects when reversing the sense of the current (joule heating is not reversing, it is always positive). Thermoelectric effects are due to the free-electron density variation with temperature amongst materials and the associated fluxes. Jordan (1980)

A typical thermoelectric module consists of pair of P-type and N-type semiconductor thermo elements is shown in fig 1.6 below forming thermocouples which are connected electrically in series and thermally in parallel.

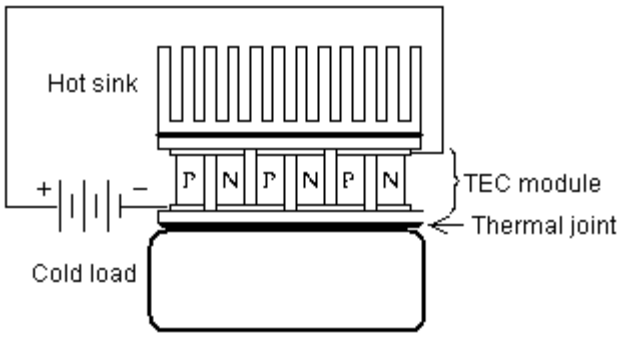


Fig. 1.6 Sketch of a thermo-electric-cooler (TEC) with three thermo-elements

1.3.6 Evaporative cooling

Mixing water and non-saturated air produces a refrigerating effect (i.e. a temperature drop below ambient temperature), is an old technique been used by ancient Egyptians to cool drinking water in porous earthen pots, and to cool space by splashing some water on the floor.

The basic refrigeration effect is due to the energy demanded by evaporating water (equal to the enthalpy of vaporisation), a natural process driven by air dryness. Related to evaporative cooling is vaporisation cooling when vacuum is applied to a liquid or solid (usually aqueous solutions).

Evaporative cooling, however, is not usually covered under Refrigeration because it is rather limited in practice to slightly cooling the water or the air that are fed to the system; it's main limitations are that evaporation is a slow process, that small inefficiencies in heat exchangers rapidly decreases efficiency of the process, water-handling is cumbersome below 0 ºC, and that moist air must be desiccated to have a continuous evaporative-cooling process. However, new developments in desiccant

regeneration are showing promise particularly for air-conditioning applications (without air desiccants, the growing humidity hinders its effectiveness). Jordan (1980)

.

1.4 STATEMENT OF THE PROBLEM

In developing countries there is a growing interest in refrigeration for food and vaccine preservation. Simple solar refrigerators working without need for electricity supply would be very valuable in rural areas where there maybe no electricity supply. Mechanical refrigerators powered by solar cells are available, but are too expensive. In the last twenty years, adsorption refrigerators using water as a refrigerant and Zeolite as an adsorber have been successfully developed.

In areas with abundant sunshine, solar radiation is the most easily accessible energy source. Solar refrigerators can work independently of the electrical network. Extensive vaccination programmes are in progress throughout the developing world in the fight against common diseases. To be effective, these programmes must provide immunization services to rural areas. All vaccines have to be kept within a strict temperature range throughout transportation and storage. The provision of refrigeration for this aim is known as the vaccine cold chain.

In Africa about 1800 solar refrigerators are used to store vaccines (WHO). Usually, refrigeration is produced by a vapour compression cycle, which is driven by electric power produced or generated by solar cells. However, the investment of about USD 2000 is high and the population cannot afford such systems, in addition, the high-tech production of solar cells seems to be difficult in developing countries Siegfried (

1.5 OBJECTIVE

Everywhere in our world refrigeration is a major energy user. In poor areas "off guide" refrigerators is actually an important need. Both of these consideration point the way toward refrigeration using renewable energy as part of a sustainable way of life.

The objective of this project is to develop a suitable grade of Zeolite as the adsorber (considered as a chemical compressor), design, construct and test a Zeolite-water solar powered refrigerator with water as the working fluid,

The solar refrigerator to be designed must be simple, cost effective, affordable and reliable.

1.6 JUSTIFICATION

The technical feasibility of solar cooling has been investigated in many countries by many researchers, using various refrigeration cycles and design as can be seen from the above review. Various degrees of successes have been achieved, which demonstrates that solar adsorption refrigeration is possible. Also the various cooling system and modifications reviewed have made use of similar solar flat plate collectors and adsorption materials such as silica gel, activated carbon and Zeolite. However, the Zeolite system is preferred as it is more cost effective and environmentally friendly

In Nigeria very little has been done in the field of solar cooling where the annual mean total solar radiation received over 24hours in Nigeria is about 210 W/ m^2 which is high enough to encourage efforts to utilize the abundant energy.

This knowledge will therefore be a basis for further work on solar cooling will be done in this university and the country as a whole. Because of limited resources, I have

placed emphasis on the use of locally available materials; to produce and appropriate type of Zeolite and the use of a parabolic trough concentrator to assist in obtaining high temperatures required for high rate of refrigerant generation. . Air cooling is adopted for the system rather than water cooling due to its availability. Solar energy is adopted because its.

- A green source of energy
- It abundant and readily available
- Cheap source of energy

Zeolite cooling on the other hand is especially suited and chosen for this solar energy application for the following reasons:

- The process uses heat during charging, and releases heat when adsorbing, making it possible to store energy by 'precharging' Zeolite for later use.
- Relatively low heating temperatures are involved and only a medium vacuum.
- Zeolite is cheap, safe, light, and re-usable
- Water is environmentally friendly, low cost, and non-toxic.

This project is thus justified by the fact that Adsorption refrigeration systems have the advantages of being environmentally benign, having zero ozone depletion potential (ODP) as well as zero global warming potential (GWP) due to the use of natural refrigerants such as water therefore making it eco-friendly. It is also attractive for the efficient use of solar energy and low-grade waste heat. Less vibration, simple control, low initial investment and expenditure, and less noise are the advantages of adsorption systems over the existing vapor compression and absorption systems.

CHAPTER TWO

LITERATURE REVIEW

2.0 INTRODUCTION

Solar cooling could be preferred in areas of the world where there is a demand for cooling due to high isolation levels, and there is no electricity supply to power conventional systems. The most promising applications are vaccine storage and food storage. Solar thermal systems for refrigeration have been studied for some years, and many refrigerators have been built and tested. Earlier work concentrated on intermittent absorption cycles such as the ammonia—water machines but more recently, solid adsorption cycles have been examined. These have the advantage of requiring no rectifiers, valves, or liquid seals such as are needed in the ammonia water cycle.

2.1 REVIEW OF PAST WORK IN THE AREA

Hildebrand et.al (2000), reported tests for a new solar powered adsorption refrigerator with high performance. The adsorption pair was silica gel / water. The machine did not contain any moving parts and did not consume any mechanical energy. Cylindrical tubes functioned both as the absorber system and the solar collector (flat plate $2m^2$ double glazed). The condenser is air cooled (natural convention). The evaporator has a capacity of 40 litres of water that can freeze. The ice functions as a cold storage for cabinet's 320 litres capacity. The first test showed a very promising performance, a cooling COP of 0.19. The paper also described the principle of the cycle, and the different component of the machine and the test procedure.

The Needful Provision Inc, (NPI) (2005) developed a simplified and improved version of solar adsorption-desorption refrigerator, developed in Germany, France and the U.S which were all characterized by no moving parts. The naturally occurring silicon components (Zeolite) were used as the absorber and water as the working fluid. The locally constructed solar refrigerator consists of a 7ft x 7ft insulated open top solar flat plate collector, a container for the Zeolites made of 6inch PVC Pipe a vacuum hand pump, heat exchanger, refrigeration box of 4cu.ft and an adapter. The refrigerator produced 5lbs of ice daily per cubic ft of storage space.

Tcherenev (1983) of the Zeo power company in his work used natural Zeolites to produce a solar refrigerator. The refrigerator produced consist of a solar Zeolite panel on the top (containing the Zeolite and surface is painted black), an air cooled condenser in the centre and a storage tank- evaporator on the bottom inside a commercial ice box. The refrigerator produced 0.9KW of cooling for each square meter of collector area and had a COP of 0.15.

Siegfried et.al (1998) in their work carried out experiment on a solar adsorption refrigerator using Zeolite and water. An experimental rig was constructed to determine the desorption temperatures which can be reached with a solar collector. The water vapour in the evaporator is adsorbed by the Zeolite and water cooled to 0^0C. The Zeolite was placed in the vacuum tube solar collector which was heated to 180^0C by artificial sunlight with a bulb type Osram HGi-T400/DH whose spectrum is similar to the solar spectrum and incident on the plane at about 300W/m^2. Typical results obtained showed that at 150^0C heating temperature there was a cooling energy of 250 KJ per kg of Zeolite and a storage volume of 125 litres could be cooled down by solar power

gained from a collector area of $3m^2$. Based on experimental data obtained a simulation of the prototype was done characterized by a $0.125m^3$ cooling chamber, a solar collector of 3 m^2 and parabolic reflectors to focus the whole incident radiation. Results generated showed that a solar irradiation of 300W/ m^2 is sufficient to reach the desorption temperature of 170^0C. The resulting cooling energy density was 350KJ/Kg Zeolite and a COP of 8%.

Miguel et.al (2003) work showed experimental evaluation of a prototype solar refrigerator based on an intermittent thermodynamic cycle of adsorption, using water as refrigerant and Zeolite as the adsorber. The system uses a mobile adsorber, which is regenerated out of the refrigeration cycle and no condenser was applied. The cold chamber has a capacity of 44litres and was used for food and vacuum storage.

Anyanwu,(2004) reviewed the basic principles and theories of solar adsorption refrigerator, the thermodynamic design and procedure for solar adsorption using activated carbon /methanol activated carbon/ammonia and Zeolite /water. They showed that Zeolite /water was the best pair for air conditioning application, while activated carbon and ammonia is preferred for ice making deep freezing and food preservation. They also show that in the above cases, the systems depend strongly on the adsorption and condensation temperature and weakly on the evaporation temperature. The maximum possible net solar COP was found to be 0.3, 0.19 and 0.16 for Zeolite/water, activated carbon/ammonium and activated carbon/methanol respectively when a conventional flat plate solar collector is used.

Anyanwu and Ogueke. (2004) presented a design, construction and test run of a solid adsorption solar refrigerator. He used activated carbon/methanol as the adsorbent/adsorbate pair. The refrigerator has three major components: collector/generator/adsorber, condenser and evaporator. Its flat plate type collector/generator/adsorber used clear plane glass sheet of effective exposed area of 1.2 m^2. The steel condenser tube with a square plan view was immersed in pool of stagnant water contained in a reinforced concrete tank. The evaporator is a spirally coiled copper tube immersed in stagnant water. Adsorbent cooling during the adsorption process is both by natural convection of air over the collector plate and tubes and night sky radiation facilitated by removing the collector box end cover plates. Ambient temperatures during the adsorbate generation and adsorption process varied over 18.5–34 °C. The refrigerator yielded evaporator temperatures ranging over 1.0–8.5 °C from water initially in the temperature range 24–28 °C. Accordingly, the maximum daily useful cooling produced was 266.8 KJ/m^2 of collector area.

2.2 CHARACTERISTICS OF THE ADSORBENT- ADSORBATE PAIR

The choice for the working fluid – the adsorbate depends on the evaporator temperature and must have a high latent heat of evaporation and small molecular dimensions to allow an easy adsorption.

Using water as refrigerant is due to its most important property its high enthalpy of vaporization (2438KJ/Kg at 25^oC). With water as adsorbate, Zeolite is a very suitable adsorbent due to its high adsorptivity property. This material is basically porous aluminium silicate that can be found raw or synthesized, is innocuous, well available and is cheap.

2.3 ZEOLITE

The term Zeolite was originally coined in the 18th century by a Swedish mineralogist named Cronstedt who observed, upon rapidly heating a natural Zeolite that the stones began to dance about as the water evaporated. Using the Greek words which mean "stone that boils," he called this material Zeolite. A commonly used description of a Zeolite is a crystalline aluminosilicate with a cage structure. Technically, we speak of a Zeolite as a crystalline hydrated aluminosilicate whose framework structure encloses cavities (or pores) occupied by cations and water molecules, both of which have considerable freedom of movement, permitting ion exchange and reversible dehydration. This definition places it in the class of materials known as "molecular sieves." [The pores in dehydrated Zeolite are 6 Ångstroms in size, while those of a typical silica gel average about 50 Å, and activated carbon averages 105 Å.]

More than 150 Zeolite types have been synthesized and 40 known naturally occurring. Zeolites occur as hydrates, and all members of the family contain at least one silicon atom per aluminum atom.

$Al_2O_3 \cdot 2SiO_2 \cdot 4.5\ H_2O$

Many Zeolites lose water fairly continuously over a temperature range of 150 to 400^{o}C without collapse of the framework structure and readsorb it from the atmosphere at room temperature. All Zeolite are molecular sieves that can selectively adsorb molecules on the basis of their size, shape or electrical charge.

Zeolites have a number of characteristic properties that are important for commercial applications including:

i. High degree of dehydration and easily dehydrated
ii. Low density and large void volume when dehydrated
iii. Stability of crystal framework structure when dehydrated.
iv. Cation exchange properties
v. Uniform molecular sized channels in the dehydrated crystals.
vi. Ability to adsorb gases and vapors.
vii. Catalytic properties with H+ exchanged forms.
viii. Special electrical properties

2.3.1 Commercial and Domestic Uses

i. Agriculture
ii. Medical
iii. Heating and refrigeration
iv. Detergents/ catalysts
v. Construction
vi. Gemstones

CHAPTER THREE

DESIGN THEORY AND CALCULATIONS

3.0 DESIGN THOERY

The concept of operation of a Zeolite solar-cooling system can be understood bystudying the fundamentals of the Zeolite-water adsorption technology. The Zeolite is placed and sealed in an air tight container irradiated by the sun. During the day cycle, the Zeolite and its container are heated to a maximum temperature of 120^{o}C. At about 40^{o}C water vapour starts desorbing from the Zeolite, and its partial pressure in the closed system starts to rise. When the pressure reaches the value determined by the condenser temperature the vapour begins to liquefy, heat is rejected to the outside, and liquid water flows into the storage tank. During the night cycle the Zeolite is cooled by convection to the ambient temperature and is ready to absorb water vapour at low partial pressures. Liquid water from the storage tank is introduced into the evaporator, where it absorbs heat from the space to be cooled and is converted into water vapour. If the partial pressure is maintained at the evaporator temperature, the water in the evaporator will boil. The Zeolite then absorbs the water vapour produced by the evaporator rejecting the heat of adsorption to the atmosphere. At the end of the night cycle, the Zeolite is loaded with all the water it can adsorb at the partial pressure of the evaporator and is ready for the beginning of a new day cycle.

A Zeolite system like any other refrigerator system has to be free of air. Therefore the Zeolite is to be placed in air tight containers which are to be painted black for maximum solar absorption, are connected through ordinary plumbing to the condenser, water storage tank and evaporator.

In a closed vessel filled with Zeolite the pressure of water vapour P_w at equilibrium is a function of the temperature T_z(K) and the water content c of the Zeolite

$$\% = \frac{(\quad)}{(\quad)} \ldots\ldots\ldots\ldots\ldots\ldots\ldots\ldots\ldots\ldots\ldots\ldots (3.1)$$

When the desorption starts the Zeolite is nearly saturated with water. "High" load c_h. The desorbed water condenses in the condenser. There the vapour pressure is equal to the saturation vapour pressure of water P_s at ambient temperature T_a. The process stops when equilibrium is reached. Then the "low" load c_l of the Zeolite causes a vapour pressure in the adsorber which is equal to the vapour pressure in the condenser.

During refrigeration the water vapour is adsorbed by the Zeolite while at ambient temperature T_a. The adsorption stops when the Zeolite is saturated containing the "high" water content c_h. At equilibrium the pressure in the adsorber is equal to the saturation vapour pressure of the refrigerant at the cold temperature T_c.

$$p\ (T) = p\ (c\ T) \ldots\ldots\ldots\ldots\ldots\ldots\ldots\ldots\ldots\ldots\ldots\ldots (3.2)$$

From this equation c_h can be calculated. In the adsorption cycle the mass of water m_w is adsorbed by the mass of Zeolite m_z is

$$= \quad (\quad - \quad) \ldots\ldots\ldots\ldots\ldots\ldots\ldots\ldots\ldots\ldots\ldots\ldots\ldots\ldots (3.3)$$

If m_w is evaporated, the refrigerant is cooled down by the cooling energy

$$= h \quad \ldots\ldots\ldots\ldots\ldots\ldots\ldots\ldots\ldots\ldots\ldots\ldots\ldots\ldots (3.4)$$

Where h=enthalpy of vaporization

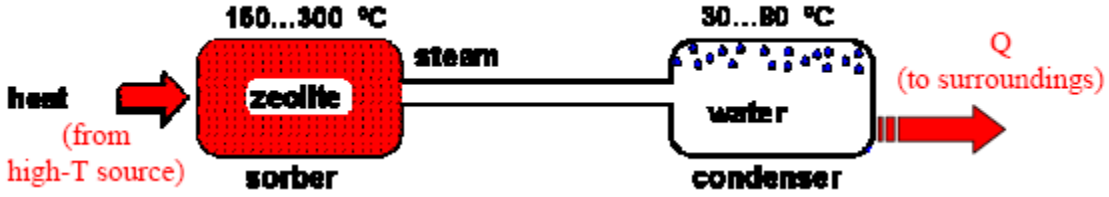
3.1 ADSORPTION CYCLES FOR SOLAR COOLING

The adsorption cycle is best understood with reference to the p-T-x (pressure-temperature concentration) diagram. An ideal cycle is presented in the Dühring diagram (Ln*P* vs. –1/*T*). This process proceeds in an evacuated (airless) environment as shown in fig 3.1a.the attraction of water by the Zeolite is so forceful that the internal pressure drops dramatically. The remaining water in an attached vessel evaporates, cools down and freezes immediately due to the heat of evaporation. The resulting ice can be used for cooling and air conditioning while the simultaneously produced heat of adsorption within the Zeolite tank can be utilized for heating. If a valve is included between the two vessels, the heat or cold production can be interrupted for any periods without loss of energy.

The first phase of this process proceeds up to the point when the Zeolite is saturated with water. The reverse process is initiated by heating the Zeolite at high temperatures in the second phase fig 3.1b. The adsorbed water molecules are forced to evaporate (desorption). Condensation takes place in the water tank (condenser). The sequence of adsorption/desorption processes is completely reversible and can be repeated indefinitely.



3.1a Adsorption phase of a Zeolite system



3.1 b Desorption phase of a Zeolite system

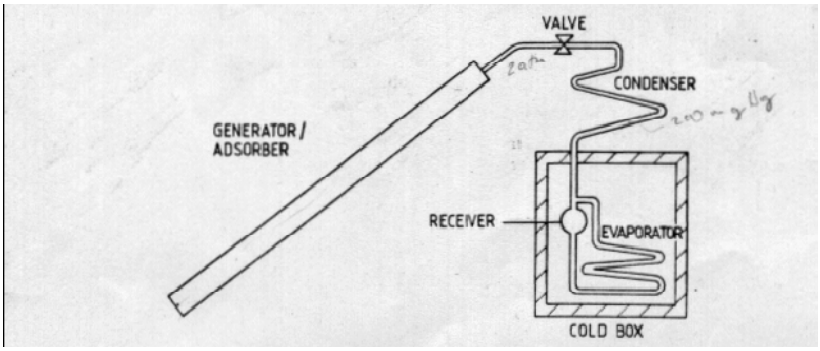


Figure 3.2 - Schematic diagram of the simple adsorption refrigerator.

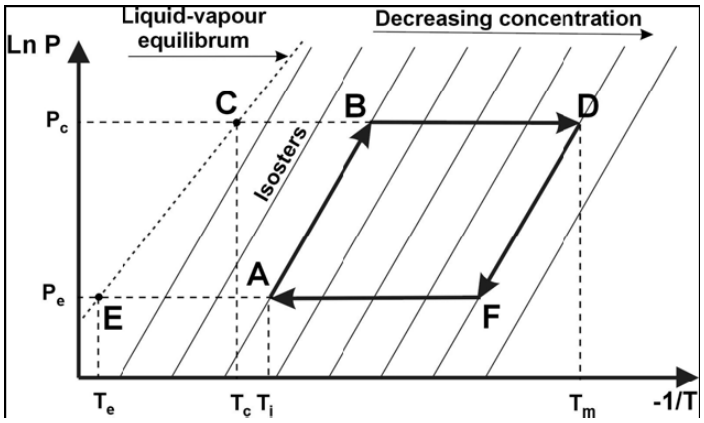
Refrigeration process entails

1. Starting in the morning with the valve open and at ambient temperature. concentration of adsorbent in the generator/absorber is heated by solar energy until the pressure reaches a level that enables refrigerant to desorb and be condensed in an air or water cooled condenser.

2. Refrigerant is driven off at constant pressure, the adsorbent becoming more and more dilute until the maximum cycle temperature*)* is reached. The condensed liquid is collected in a receiver.

3. The valve is shut, and the adsorbent cools and reduces its pressure. At some stage of the evening or night its pressure will be the saturated vapor pressure of refrigerant which is sufficiently low for ice production.

4. The valve is now opened, and the liquid refrigerant starts to boil in the evaporator. Initially the Refrigerant within the evaporator and receiver simply cools itself, but having dropped below condenser temperature it can start to freeze water. Adsorption is completed by the following morning, completing the cycle. During this process heat is released in the absorber and so the generator/absorber must be cooled be ambient temperature air or water.



LEGEND

Saturation liquid-vapour curve for the refrigerant (EC dashed line), isoster curves (thin lines), adsorption cycle (thick lines). Heating period : step AB (7 a.m.→10 a.m.) and step BD (10 a.m.→4 p.m.) ; cooling period : step DF (4 p.m.→7 p.m.) and step FA (7 p.m.→7 a.m.).

Fig 3.3: An ideal adsorption cooling cycle (Duhring diagram)

The cycle is explained in detail (7) we can summarize in four stages:

Step 1: Isoteric heating (A→B): The system temperature and pressure increase due to the solar irradiance.

Step 2: Desorption and condensation (B→D): Desorption of the water steam contained in the Zeolite: condensation of the water steam in the condenser; the water in the evaporator is drained through the valve.

Step 3: Isoteric cooling (D→F): Decrease in period of sunshine; cooling the adsorbent; decrease of the pressure and temperature in the system.

Step 4: Adsorption and evaporation (F→A): Evaporation of water contained in the evaporator; cooling of the cold cabinet; production of ice in the evaporator: readsorption of water steam by the Zeolite

3.2 DESIGN CONSIDERATIONS OF THE COOLING SYSTEM

3.2.1 Initial data

Ambient temperature (outside) - $32^{o}C$

Ambient room temperature - $26^{o}C$

Required cold box temperature - $5^{o}C$

Condenser design temperature - $30^{o}C$

Evaporator design temperature - $2^{o}C$

Regenerative temperature - $50^{o}C – 250^{o}C$

3.2.2 Design dimensions for the cold box

Length of box = 0.4m = 40cm

Width of box = 0.3m = 30cm

Depth of box = 0.3m = 30cm

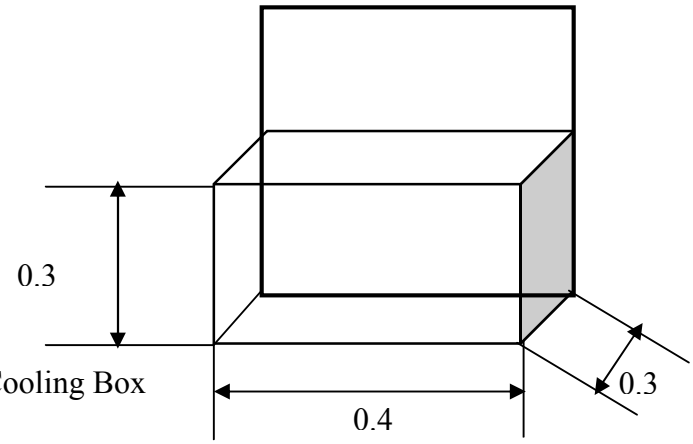


Fig 3.4: Cooling Box

3.3 HEAT LOAD CALCULATION

Heat load or refrigeration load is the rate at which heat must be removed from the cold box in order to produce and maintain the desired temperature conditions.

(a) Wall heat gain load: cold box wall conduction is from the following materials, galvanized iron, fibre (insulation) and aluminium for the evaporators.

The wall heat gain is given by:

$Q = AU\Delta Q$ ..... (3.5)

Where $\frac{1}{U} = \frac{1}{f_0} + \sum_{i=1}^{n} \frac{X}{K} + \frac{1}{f_i}$ ..... (3.6)

U = overall heat coefficient

f = cooling factor

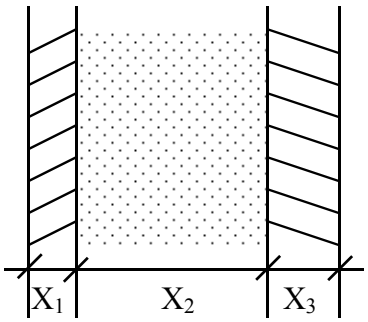


Fig. 3.5: Cross – section of cooling box

Thickness of galvanized iron, $X_1 = 1 \times 10^{-3}$m

Thickness of insulation, $X_2 = 25.4 \times 10^{-3}$m

Thickness of aluminium, $X_3 = 1 \times 10^{-3}$m

Cooling factor rate, $f_0 = 68.2 \times 10^{-4}$ KW/m^{2}K

Cooling factor rate, $f_i = 227.1 \times 10^{-4}$ KW/m^{2}K

Thermal conductivity of G.I, $K_1 = 65$W/mK

Thermal conductivity of fibre, $k_2 = 0.04$W/mK

Thermal conductivityof Aluminium, $k_3 = 205$W/mK

But **Q** = AUΔT

A = Outside heat transfer area

ΔT = Temperature difference between outside and cold box exterior plus a temperature allowance for solar radiation.

Refrigeration load allowance for solar radiation where

0, 3, 4, 4, 4, are solar temperature allowances for N, S. E, W respectively.

$Q_{walls} = Q_N + Q_S + Q_E + Q_W$

3.4 PRODUCT LOAD

Product load is usually calculated for a 24-hour period. Not only must the product itself be cooled but, the containers as well. Product cooling load is calculatedas follows:

Product load = lbs of product + container x specific heat x temp. difference

The cooling box has a volume of 0.036m^3 which is capable of storing 36litres of water.

$$Q_p = \frac{W \times C_p (T - T_{freeze})}{T \times f} \quad \text{.....(3.9)}$$

3.5 USAGE LOAD

The heat usage or service load is the sum of the heat loads of: cooling the contents to cabinet temperature; cooling of air changes; removing field and respiration heat from fresh produce; removing heat released from electrical lights and motors; and removing heat given off by people entering and/or working in the storage room per unit of time (usually 24 hours).

3.6 DESIGN OF THE EVAPORATOR

The evaporator should be made from very high conducting material of copper.

For a copper pipe with standard dimensions:

Outer diameter D = – = 9.375 x 10^{-3}m

Outer Radius R = — = 4.688 x 10^{-3}m

Inner diameter, d = – = 6.25 x 10^{-3}m

Inner radius, r = – = 3.125 x 10^{-3}m

$Q_{evaporator} = Q_{Total\ cooling\ load}$

Heat transfer by conduction through the walls of the evaporator is given as

$$Q_{Evaporator} = 2\pi rLh_i(t_i - t_o) = \frac{2\pi L(t_R - t_E)}{\frac{Ln\,R/r}{K} + \frac{1}{Rh_o}} \quad \text{.....(3..10)}$$

Where L = length of coil

To obtain h_i we note the Chato-equation for evaporation inside the tube can be used

$$Nu = 0.555\left[g\rho_v \frac{(\rho_L - \rho_V)d^3 h_{fg}}{\mu_r k_v \Delta T} \right]^{1/4} \quad \text{.....(3.11)}$$

$$Nu = \frac{h_i d}{k_v} \quad \text{.....(3.12)}$$

/

$h =$ ——

$Q = 2\pi rLh_i(t_R - t_E)$

$=$ ——————

2 $h($ $-$ $)$

3.7 DESIGN OF THE CONDENSER

Condenser will be a base wire coil – end – air type. Heat transfer for cooling the condenser is by natural convection to the ambient air.

Across the walls of the condenser heat transfer is given by:

$$Q = m(h_2 - h_1) = 2\pi rLh_i\,(t_R - t_C) = \frac{2\pi L(t_R - t_C)}{Ln\frac{R/r}{k} + \frac{1}{Rh_o}} \quad \text{.....(3.13)}$$

For condensation inside a cylindrical tube we note that after comprehensive work and experimental investigation, Akers, Deans and Crosses reported that for both horizontal and vertical tubes the following convection equation hold true:

For $Re_d < 5x10^4: Nu_d = 5.03 Re_d^{1/2} Pr^{1/3}$ .....(3.14)

$Re_{d>} 5x10^{4:} Nu_d = 0.0265 Re_d^{0.8} Pr^{1/3}$ .....(3.15)

= — ..... (3.16)

For these correlations G, the equivalent mass velocity is defined as:

$$G = G_L + G_v \left(\frac{\rho_L}{\rho_v} \right)^{1/2}$$ .....(3.17)

G_L and G_v are mass velocities (mass flow rate per unit cross-section area) of the full pipe on the tube of liquid and vapour phases.

$$G = \frac{M_L}{A} + \frac{M_v}{A} \left(\frac{\rho_L}{\rho_v} \right)^{1/2}$$ .....(3.18)

Considering for a base coil – end – air type, heat transfer for cooling the condenser by free convection to the ambient air, $Q = hA\Delta T$

Where

h =

=

For simplified relations for boiling, heat transfer coefficients to water at atmospheric pressure

For horizontal tubes

– / < 16

$hW/m^2\,{}^oC = 1042(\Delta T_2)^{2/3}$ approximate range = 0.776

Approximate range of G, $W/m^2\,{}^oC = 0 – 2060$

For film condensation inside horizontal tubes, Chato equation holds

$$h = 0.555\left[\frac{S_L(\rho_L - \rho_v)gk^3 h_{fg}}{\mu d(T_g - T_w)}\right]^{1/4} \quad \text{.....(3.19)}$$

This equation is restricted to low vapour, Reynolds such that

$$= \qquad / < 35{,}000$$

Re_v is evaluated at inlet conditions to the tube. For higher flow rates an approximate expression is given by Akers, Deans and Crosses as

$$\frac{\text{hd}}{\text{k}} = \qquad 0.026 \ \bar{} \ \text{Re}0.8 \ldots\ldots\ldots\ldots\ldots\ldots\ldots (3.20)$$

$$\text{Re}_m = \frac{d}{\mu_f}\left[G_f + G_v\left(\frac{\rho_f}{\rho_v}\right)^{\frac{1}{2}}\right] \quad \text{.....(3.21)}$$

$G_{f\,(Liquid)}$ and $G_{v\,(vapour)}$ are calculated as if each occupies the entire flow area.

3.8 COLLECTOR DESIGN

The collector used will be a parabolic trough concentrator and is designed for all year round performance. Performance of April (one of the months with high (irradiance)) and July (month with the lowest irradiance) will be only estimated. The mean annual solar irradiance for Zaria is taken as 280.4W/mK, Bala (1980)

3.8.1 Design of the Parabolic Trough

The equation of a parabola is given by $x^2 = 4ay$ in Cartesian co-ordinates, with origin at the focus and in polar co-ordinates with the origin at the focus is:

$$= \frac{2}{1 - \qquad} \equiv \frac{\qquad}{\emptyset \qquad \emptyset} \ldots\ldots\ldots\ldots\ldots\ldots\ldots\ldots\ldots\ldots\ldots\ldots\ldots\ldots\ldots\ldots (3.22)$$

where r is the distance from the origin

f is the focal length

Ø is the angle between the radius and the horizontal axis

3.8.2 Design requirements for concentrators

Concentrators are needed whenever we want to use solar power for application requiring heat at temperatures above about 80^{o}C as provided by flat plate collectors. There are numberless applications requiring temperatures up to about 300^{o}C for both domestic and industrial applications like space cooling, cooking, desalination and electricity generation. Factors that influence the design of concentrators of solar energy are:

i) Cost and ease of manufacture

ii) Extent of guidance required for following the sun

iii) Durability and maintenance

iv) Required working temperature of the absorber

v) Preferred geometry of absorber in relation to the model of utilization of the energy

vi) Susceptibility to contamination and durability under UV radiation.

3.8.3 Collector sizing

Once the energy delivery requirements for a collector field are established, other factors must be considered. For a given energy delivery requirement at a specified temperature,

the flow rate is established. Heat transfer into the working fluid at a given flow rate is a function of the diameter and it is not linearly proportional.

To a limit the energy transfer into the working fluid is enhanced by a smaller receiver diameter. Since this is the case the collector aperture can be adjusted to achieve the proper receiver diameter to optimize the collection efficiency. It must be kept in mind that the energy delivered is energy collected less energy required to drive the fluid through the collector system.

3.8.4 Receiver Tube Diameter

In a tactual approximation for the sizing of the receiver tube diameter, the assumption can be made that it is appropriate to attempt to capture all the energy reflected from the parabola.

The receiver tube size would then be dependent upon the sun's angular width, the magnitude of the tracking error, the mirror error (i.e. the departure from a tangent to a theoretical parabola), the irregularity of the reflective surfaces and the angular absorptance characteristic of the solar coating.

$$\text{Receiver tube diameter} = \frac{2 \quad -}{60 \sin(\quad)} \ldots\ldots\ldots\ldots\ldots\ldots\ldots\ldots\ldots\ldots (3.23)$$

Figure 3.6 sums these influencing factors in a conservative arithmetic manner since the potential magnitude of tracking and slope errors is not completely known. From this figure since the sizing is in terms of angular aperature, it can be seen that the receiver diameter is proportional to the distance from the reflector.

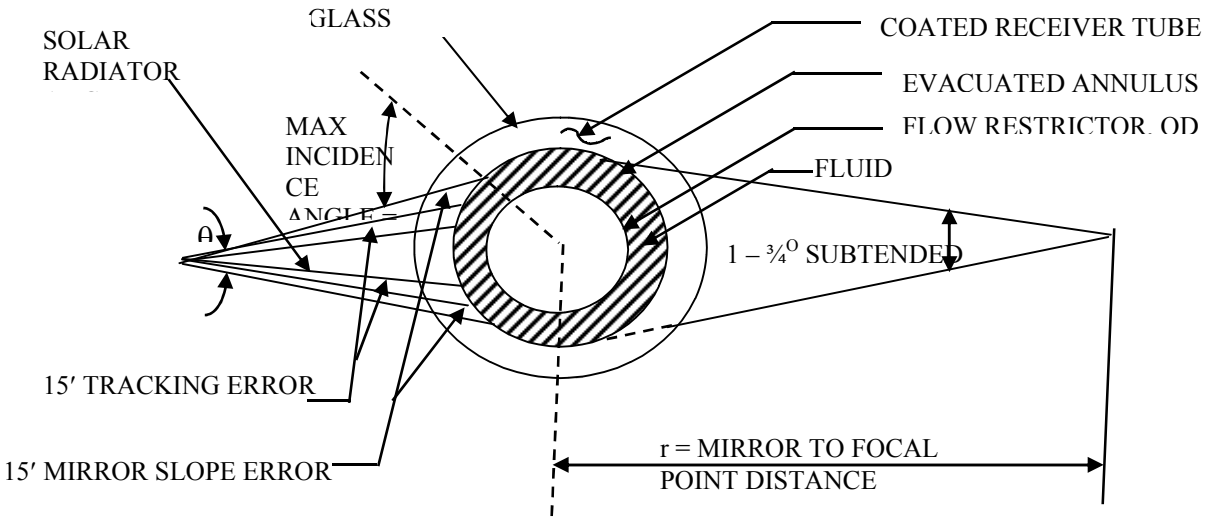


Fig 3.6: Thermal Losses Proportional to Receiver Tube Diameter

Thermal losses are directly proportional to the receiver diameter. so the obvious goal is to select a parabolic rim angle which would result in the smallest maximum distance from parabola to focus. A table showing suitable pipe diameter for different rim angles and collector sizing is shown in appendix A.

3.9 ENERGY BALANCE FOR THE PARABOLIC TROUGH CONCENTRATOR

The energy balance includes direct normal solar radiation incident on the collector, optical losses from both the collector and heat collection element (HCE) and the heat gain into the heat transfer fluid (HTF).

3.9.1 **One dimensional energy balance model**

For short receivers (<100m) an energy balance between the heat transfer fluid (HTF) and the atmosphere includes all equations and correlations necessary to produce the terms of the energy balance which depends on the collector type, Heat Collector Element(HCE) condition, optical properties and ambient condition.

Fig. 3.7 shows a one dimensional steady-state energy balance for a cross-section of an HCE with and without the glass envelope.

Fig.3.8 shows the thermal resistance model and subscript definitions.

For clarity, the incoming solar energy and optical losses are omitted from the resistance model. Optical losses are due to imperfections in the collector mirrors tracking errors, shading and mirror and the HCE cleanliness.

The effective incoming solar energy = (solar energy – optical losses) is absorbed by the glass envelope = $q'_{5sol\ Abs}$. The absorber coating (selective) = $q'_{3sol\ Abs}$

Some energy that is absorbed into the selective coating is conducted through the absorber $q'_{3sol\ Abs}$ and transferred to the heat transfer fluid by convection q'_{34} and radiation $q`'_{34}$ and through the HCE support brackets through conduction tend bracket.

The energy from the radiation and convection then passes through the glass envelope by conduction ($q'_{34\ cond}$) and along with the energy absorbed by the glass envelope ($q'_{5sol\ Abs}$) is lost to the environment by convection (q'_{5conv}) and radiation ($q'_{5sol\ rad}$).

If the glass envelope is missing, the heat loss from the adsorbed is lost directly to the environment.

This model assumes all temperatures, heat flames and thermodynamic properties are uniform around the circumference of the HCE.

With the help of Fig 3.7 the energy balance equations are determined by considering energy at each surface of the HCE cross-section with and without the glass envelope. Heat lost to the surrounding by convection = q'_5

If a glass envelope was used to enclose the heat collector element – energy from the radiation and convection, then passes through the glass envelope = $q'_{45\ cond}$.

Energy absorbed by the glass envelope = $q'_{5sol\ Abs}$. With the glass envelope.

$$q``'_{12conv} = q'_{23cond} \quad \text{.....(3.24)}$$

$$q'_{3sol\ Abs} = q'_{34\ conv} + q'_{34'\ cond} + q'_{23cond} + q'_{cond,\ bracket} \quad \text{.....(3.25)}$$

$$q'_{34\ conv} + q'_{34\ rad} = q'_{45cond} \quad \text{.....(3.26)}$$

$$q'_{45cond} + q_{5sol\ abs} = q``_{56onv} + q'_{57\ rad} \quad \text{.....(3.27)}$$

$$q'_{Heat\ loss} = q``_{56conv} + q'_{57rad} + q``'_{cond,\ bracket} \quad \text{.....(3.28)}$$

Without the glass envelope,

$$Q``'_{12\ conv} = q'_{23\ cond}$$

$$q'_{3\ sol\ abs} = q``'_{36} + q``'_{57rad} + q``'_{23\ cond} + q'_{conv\ bracket} \quad \text{..... (3.29)}$$

$$q``'_{Heat\ loss} = q``'_{56conv} + q``'_{57rad} + q'_{cond\ bracket} \quad \text{..... (3.30)}$$

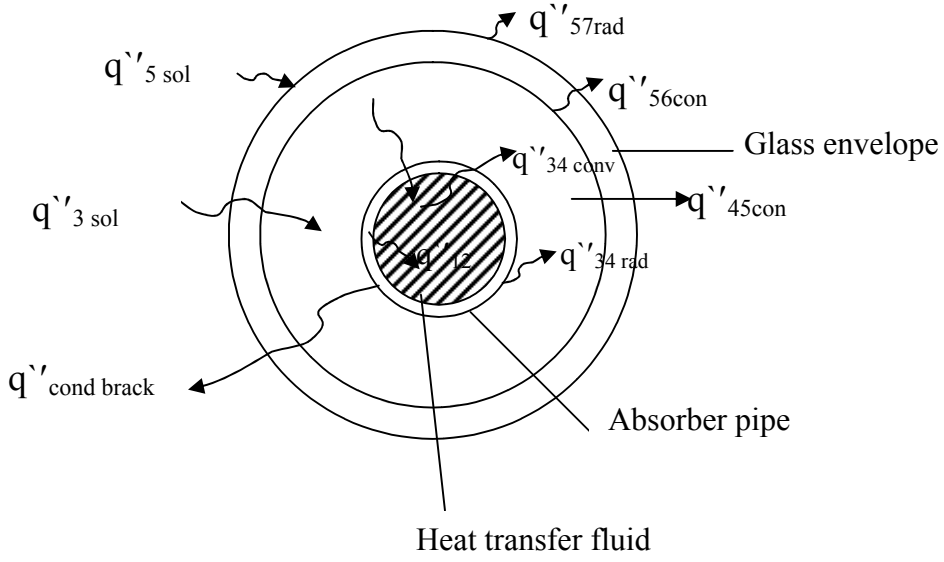


Fig 3.7:(a) Energy balance (with glass envelope)

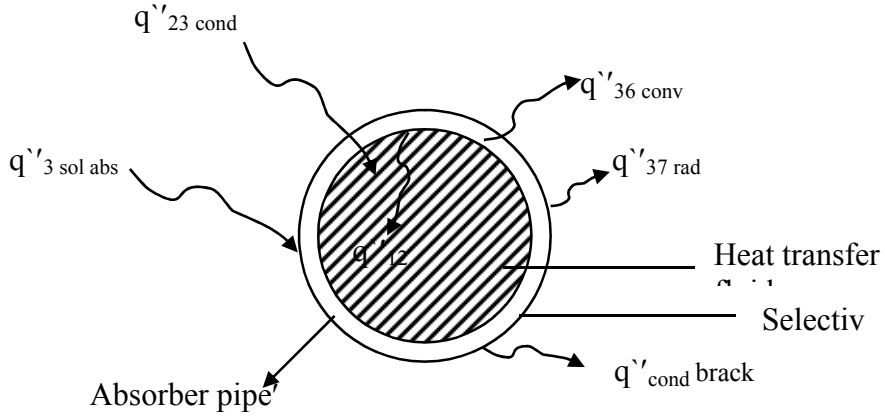


Fig. 3.7 (b): Energy balance without glass envelope

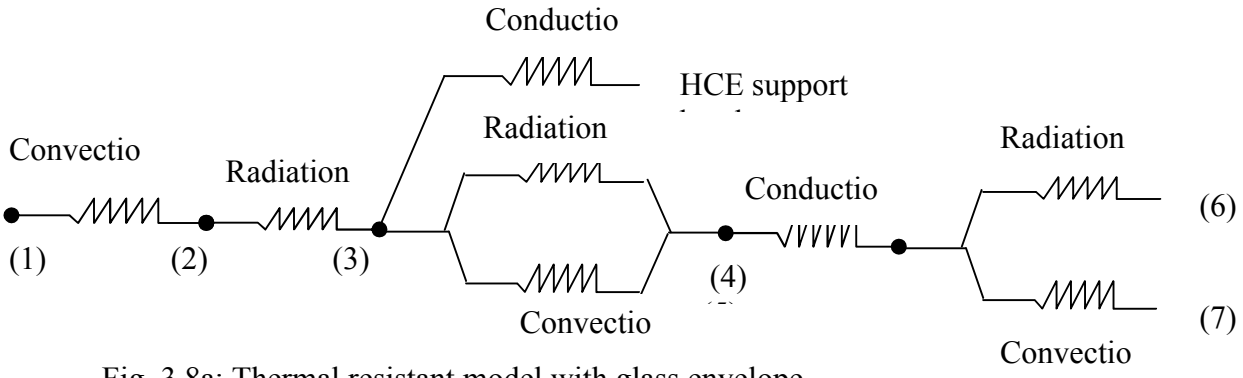


Fig. 3.8a: Thermal resistant model with glass envelope

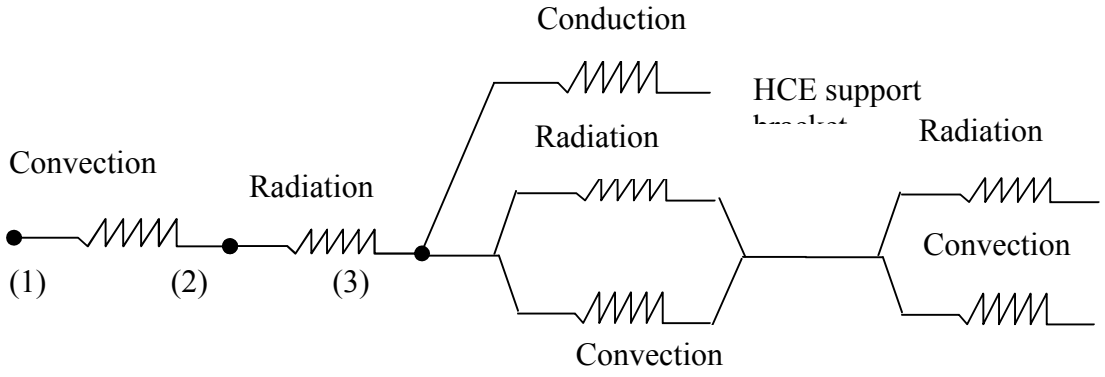


Fig. 3.8b: Thermal resistant model without glass envelope

1) Heat transfer fluid 2) Absorber inner surface 3) Absorber outer surface 4) Glass envelope 5) inner surface 6) Glass envelope outer surface 7) Surrounding sky

3.9.2 Convection Heat Transfer between HTF and the Absorber

From Newton's law of cooling the convection heat transfer from the inside surface of the absorber pipe to the HTF is:

$Q'_{12\,conv} = h_1 D_2 \pi (T_2 - T_1)$, …….(3.31)

$h =$ ———

h_1 = HTF convection heat transfer coefficient at T1 W/m^2K

D_2 = inside diameter of the absorber pipe

T_1 = Mean (Bulk) temperature of heat transfer fluid (^oC)

T_2 = Inside surface temperature

N_{uD2} = Nusselt number based on D_2

K_1 = Thermal conductance of the HTF at T_1 (W/m^2K)

Nusselt number depends on the flow from the heat collector element.

At typical operating conditions, the flow in an HCE is well within the turbulent flow region. However, during solar hours or when evaluating the HCE may become laminar because of the viscosity of the heat transfer fluid at lower temperatures. Therefore to model the heat losses under all conditions the model includes conditional statements to determine the type of flow.

The Nusselt number used for each flow condition is outlined below.

(a) Turbulent and transitional flow cases

To model the convective heat transfer from the absorber to the HTF for turbulent and transitional cases (Reynolds No > 2300) the following Nusseltt number correlation developed by Linie Linskic (1976).

$$Nu_{D2} = \frac{f_2/8\,(\mathrm{Re}_{D2}-1000)\mathrm{Pr}_1}{1+12.7\sqrt{F_2/8\,(\mathrm{Pr}_1-1)}}\left[\frac{\mathrm{Pr}_1}{\mathrm{Pr}_2}\right]^{0.11} \quad \text{.....(3.32)}$$

where

$f_2 = (1.82\log_{10}\mathrm{Re}_{D2} - 1.64)^{-2}$ = friction factor for the inner surface of the absorber

$\mathrm{Pr}_{½}$ = Prandtl number evaluated at the HTF temperature T_1 & T_2

$0.5 < \mathrm{Pr}_1 < 2000$ and $2300 < \mathrm{Pr}_2 < 5E6$

Nu = constant = 4.36 pipe flow [Incopera & Dari H, 1990]

3.9.3 **Conduction heat transfer through the absorber wall**

Fourier law of conduction through a hallow cylinder describes the conduction heat transfer through the absorber wall.

$q'_{23cond} = 2\pi k_{23}\,(T_2 - T_3)/\ln\,(D_3 - D_2)$…… (3.33)

K_{23} = Absorber thermal conductance at average absorber temperature

T_2 = Absorber Inside surface température (K)

T_3 = Absorber outside surface temperature (K)

D_2 = Absorber inside diameter (m)

D_3 = Absorber outside diameter (m)

K_{23} = (0.013) T_{23} + + 15.2 if the copper K_{23} = 400W/m^{2}K

3.9.4 **Convective heat transfer**

The two heat transfer mechanisms are evaluated to determine the convection heat transfer between the absorber and glass envelope q`′$_{34conv}$

$$\dot{}'_{34} \quad = \quad {}_3h_{34}(\ {}_3 - \ {}_4) \quad \text{.....(3.34)}$$

$$h_{34} = \frac{}{{}_3/2\ln(\ {}_4/\ {}_3 + \quad h(\frac{3}{4} + 1)} \quad \text{.....(3.35)}$$

3.9.5 **Radiation heat transfer**

Radiation heat transfer between the absorber and glass envelope (q`′$_{34rad}$) is estimated with the following equation Forristall. (2003)

$$q'_{34rad} = \frac{\sigma\pi D_2\left(T_3^4 - T_4^4\right)}{\frac{1}{\varepsilon_3} + \frac{(1-\varepsilon_4)D_3}{\varepsilon_4 D_4}} \quad \text{.....(3.36)}$$

3.9.6 Optical Properties

List of terms used to estimate he effective optical efficiencies table were generated from data published in a report by NREL (Price *et al*, 2002). Data in the table are valid only for solar incident irradiation normal to the collector aperture.

Table 3.1 estimates the effective optical efficiency terms

ε_1 = HCE shadowing (bellows shielding supports) - 0.978

ε_2 = Tracking error - 0.994

ε_3 = Geometry error - 0.98

ρ_u = Clean mirror reflectance - 0.935

ε_4' = Dirt on mirrors - ————

ε_5' = Dirt on HCE - $1 + \varepsilon_r^{½}$

ε_6' = Unaccounted - 0.96

Reflectivity is a user input typically between 0.88 – 0.93

Solar irradiation absorption in the glass envelope

$q'_{5sol\ abs} = q``'_{si}\eta_{env}\alpha_{env}$ ……..(3.37)

$\eta_{env} = \varepsilon_1\varepsilon_2\varepsilon_3\varepsilon_4\varepsilon_5\varepsilon_6\rho_{in}k$.....(3.38)

q'_{si} = solar irradiation per receiver length W/m

η_{env} = effective optical efficiency at the glass envelope

α_{env} = absorptance of the glass envelope

K = incidence angle modifier

3.9.7 **Solar irradiation absorption in the absorber**

Solar energy absorbed by the absorber occurs very close to the surface. It is treated as heat flux.

$q``'_{5sol\ abs} = q``'_{si}\eta_{abs}\alpha_{abs}$ ..... (3.39)

$\eta_{abs} = \eta_{env}\tau_{abs}$

(d) Heat loss (bracket)

$$q`'_{\text{cond bracket}} = \sqrt{h_b p_b k_b A_{cs,b}\left(\frac{T_{back} - T_b}{L_{HCE}}\right)} \quad \text{.....(3.40)}$$

h_b = Average convection coefficient of bracket (W/m^2K)

p_b = perimeter of bracket (m)

k_b = Conduction coefficient (W/m^2K)

$A_{cs,b}$ = Minimum at the base of the bracket

T_{base} = Temperature at the base of the bracket

L_{HCE} = length of heat collector element

3.9.8 No Glass Envelope Case

When the glass envelope is missing the five energy balance equation collapses down to 3; $q`'_{12conv}$ and $q`'_{3\ cond}$ remains unchanged for the 2 cases.

Also the solar absorption term for the absorber is adjusted to account for the solar flux that is no longer lost with the glass envelope.

$$\eta_{abs} = \eta_{env}$$

without ε_5 term which is accounted for particular matter on the heat collector element.

Therefore,

$$q`'_{12conv} = q`'_{23cond} \text{.....(3.41)}$$

$$q`'_{3sol,\ abs} = q`'_{56conv} + q`'_{57rad} + q`'_{23cond} + q`'_{12cond\ bracket} \text{.....(3.42)}$$

$$q`'_{Heat\ loss} = q`'_{56conv} + q`'_{37\ rad} + q`'_{cond\ bracket} \text{.....(3.43)}$$

$$q`'_{12conv} = h_1 D_2 \pi (T_2 - T_1) \text{.....(3.44)}$$

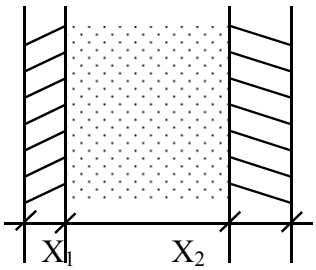
$$Nu_{D2} = \frac{f_2/8\,(\mathrm{Re}_{D2} - 1000)\mathrm{Pr}_1}{1 + 12.7\sqrt{F_2/8\,(\mathrm{Pr}^{2/3} - 1)}}\left[\frac{\mathrm{Pr}_1}{\mathrm{Pr}_2}\right]^{0.11} \quad \text{.....(3.45)}$$

$f_2 = (1.82\log_{10}\mathrm{Re}_{D2} - 1.64)^{-2}$ .....(3.46)

T_1 = mean bulk temperature of HTF

Nu_{D2} = constant = 4.36 pipe flow [Incopera & Dewitt, 1990]

3.10 DESIGN CALCULATIONS

Initial data	Design calculation	Results
$X_1 = 1 \times 10^{-3}$m $X_2 = 25.4 \times 10^{-3}$m $X_3 = 1 \times 10^{-3}$m $f_0 = 68.2 \times 10^{-4}$ KW/m^{2}K $f_i = 227.1 \times 10^{-4}$ KW/m^{2}K $K_1 = 65$W/mK $k_2 = 0.04$W/mK $k_3 = 205$W/mK	HEAT TRANSFER THROUGH COOLING BOX  $\frac{1}{U} = \frac{1}{f_0} + \sum_{i=1}^{n}\frac{X}{K} + \frac{1}{f_0} = \frac{1}{f_0} + \frac{X_1}{K_1} = \frac{X_2}{K_2} + \frac{X_3}{K_3} + \frac{1}{f_i}$ $\frac{1}{U} = \frac{1}{68.2x10^{-1}} + \frac{1x10^{-3}}{65} + \frac{25.4x10^{-5}}{0.04} + \frac{1x10^{-3}}{205} + \frac{1}{222x10^{-1}}$	$\frac{1}{U} = 0.8256$ $U = 1.2112 W/mK$
$T_{amb} = 32^oC$ $T_{con.} = 5^oC$	HEAT TRANSFER THROUGH THE 4 WALLS Refrigeration load allowance for solar radiation where 0, 3, 4, 4, 4, are solar	

	temperature allowances for N, S. E, W respectively Q_N = 0.3 x 0.3 x 1.2112 {(32-5) + 0} = 3.924288W Q_S = 0.4 x 0.3 x 1.2112 {(32 - 5) + 3} = 4.36032W Q_E = 0.3 x 0.3 x 1.2112 {(32 – 5) + 4} = 0.10901W Q_W = 0.3 x 0.4 x 1.2112 {(32 – 5) + 4} = 0.10901W $Q_{walls} = Q_N + Q_S + Q_E + Q_W$ 3.924288 + 4.36032 + 0.10901 + 0.10901	= 8.50263W
	HEAT GAIN THROUGH ROOF Q_{roof} = 0.40 x 0.30 x 1.2112 {(32 – 5) +0} = 5.377728W	Q_{roof} = 5.377728W
	HEAT GAIN THROUGH THE FLOOR OR BOTTOM Q = AUΔT	$\frac{1}{U_{floor}} = 0.78192$ $U_{floor} = 1.279394W / mK$ Q_{floor} = 3.2224072W

	$\frac{1}{U_{floor}} = \frac{1}{f_i} + \frac{X_1}{K_1} + \frac{X_2}{K_2} + \frac{X_3}{K_3}$ $\frac{1}{U_{floor}} = \frac{1}{68.2x10^{-4}} + \frac{1x10^{-3}}{65} + \frac{25.4x10^{-3}}{0.04} + \frac{1x10}{227.1x}$ Q_{floor} =0.4 x 0.3 x 1.27939 (26 - 5)	
C_{water} =4.2J/kg ρ_{water}= 1000kg/m^3 f = 0.70 $Time_{cooling}$ = 18hours Cooling temperature 5^{o}C	PRODUCT LOAD The cooling box has a volume of 0.036m^3 which is capable of storing 36litres of water. $Q_p = \frac{WxC_p(T - T_{freeze})}{Txf}$ $Q_p = \frac{20x4.2x(26-5)}{18x3600x0.7}$	$Q_p = 0.04W$
Internal dimensions of the cold box l′ = 0.364m w′ = 0.246m	USAGE LOAD Volume of box (internal) = 0.364 x 0.246 x 0.273 = 0.02326608m^3= 0.8606143ft^3 Temperature difference between the inside and outside of the cooler = 32 – 5 = 27^{o}C	

h′ = 0.273m	From reference (1) Table for usage load: $0.8606143ft^3 < 20ft^3$ The usage load = 410.66W Usage load = $\frac{0.8606143ft^3 \times 410.66}{24}$ =14.726W	Usage load=14.726W
$Q_p = 0.04W$ Q_{floor}=3.2224072 W Q_{roof}= 5.377728W Usage load=14.726W	TOTAL COOLING LOAD Q_{Total} = 8.50263 + 3.22407 + 5.3777728 + 14.276 + 0.04 = 31.4210W Considering a 10% factor of safety Q_{Total} = 34.563133W	Q_{Total} = 34.563133W
D= 3/8in= 9.375 x 10^{-3}m R = 3/16in = 4.688 x 10^{-3}m d = ¼ in = 6.25 x 10^{-3}m r = 1/8 in = 3.125	DESIGN OF THE EVAPORATOR $Q_{evaporator} = Q_{Total\ cooling\ load}$ $Q_{Evaporator} = 2\pi rLh_i(t_i - t_o) = \frac{2\pi L(t_R - t_E)}{\frac{Ln\,R/r}{K} + \frac{1}{Rh_o}}$ $Nu = 0.555\left[\frac{9.81x5.56x10^{-3}(0.0244-5.56x10^{-3})(6.25x10^{-3})(24959x10^{-3})}{8.56x10^{6}x167x10^{6}x24}\right]^{1/4}$	Nu =2.039930251 x 10^{-3} Length of evaporator = 18.124m

x 10^{-3}m For the refrigerant at the temperature of the condenser and vapour at evaporator temperature ρ_{liquid}=0.02437kg /m^3 ρ_{vapor} = 5.5586x x 10^{-3}kg/m^3 ρ_{fg} = 2495.9kg/m^3 $\mu_v = 8.56 \times 10^6$ $k_v = 16.7 \times 10^6$	$h =$ —— $h_i = 5.364855036 \times 10^{-3}$kW/$m^2$ $Q = 2\pi r L h_i(t_R - t_E)$ $L = \frac{Q}{2\pi r h_i(t_R - t_E)}$ $= \frac{34.58851}{2\pi r \times 31.6394565 \times 1.6 \times 10^{-3} \times 6}$ = 18.12390337m	
$G_{f\,(Liquid)}$ and $G_{v\,(vapour)}$ are calculated as if each occupies	LENGTH OF CONDENSER $Q = 2\pi h r_i L \Delta T$ $h = 0.555\left[995.8\frac{(995.8-963.2)x9.81x(0.678)^3 x1042x10^3}{3.06x10^6 x1.6x10^{-3} x2}\right]^{1/4}$	

the entire flow area. For water vapor at 93.33^{o}C ρ_v = 963.2kg/m^3 μ = 3.06 k = 0.675kW/m^2 Pr = 1.90 ρ_L = 995.8kg/m^3 r = 1.6 x 10^{-3}m h_{fg} = 1042kJ/kg	h = 31.63945649w/m^2 L = $\frac{\quad}{\pi \quad \Delta} = \frac{\quad \cdot \quad}{\times \quad . \quad \times \times \times}$ L = 13.12390337m	L = 13.12390337m
Nu_{D2} = constant = 4.36 pipe flow t_a = 36^{o}C t_b = 150^{o}C S = 11^{o}11′ = 11^{o}18′	CONDUCTION THROUGH ABSORBER PIPE $q_{46\ cond}$ = 3.176646 x 10^{-1} x π x 25.4 x 10^{-4} x (91 - 36) = 1.3722122564 kW $q`'_{46\ rad} = \sigma D_4 \pi \alpha_5 (T_4 - T_7)$ = 25.4 x 10^{-3} x 5.6704 x 10^{-4} x π x 0.9 (91 – 36) = 2.204449364 X 10^{-3}Kw $q'_{cond\ bracket}$ is negligible as compared to	h_c=0.31766461kW/m^2

P_1 = 3.178 bar ρ = 61.02kg/m^3 μ = 0.0271 k_g = 0.01213kW/m^3 T_1 = mean bulk temperature of HTF Nu_{D2} = constant = 4.36 pipe flow t_a = 36°C t_b = 150°C S = 11°11′ = 11°18′ Properties of fluid at a temperature between that of the absorber pipe and	the heat transfer of the system for very good insulation. $q`'_{total\ (conc)} = q`'_{23\ cond} + q`'_{12conv} + q`'_{3\ sol,abs} + q_{radcond\ brack}$ $= 0.71664 \times 3 + 2\{1.37221 + 2.204493 \times 10^{-3}\} = 5.16382922kW$ Properties of fluid at a temperature between that of the absorber pipe and ambient air. $q`'_{12conv} = h_1 D_2 \pi (T_2 - T_1)$ $Nu_{D2} = \frac{f_2/8\,(Re_{D2} - 1000)Pr_1}{1 + 12.7\sqrt{F_2/8}\,(Pr^{2/3} - 1)}\left[\frac{Pr_1}{Pr_2}\right]^{0.11}$  $f_2 = (1.82\log_{10}Re_{D2} - 1.64)^{-2}$ $h = \frac{4.36 \times 400}{25.4}$ $= 69{,}760$ / $q`'_{12conv} = 69{,}760 \times 9.375 \times 10^{-3} \times \pi \times 30$ $= 716.6450368w/m^2 = 0.7167kW/m^2$ $q`'_{12conv} = q`'_{23cond} = 0.7167kW/m^2$ $q_{46conv} = h_{46}\pi D_4 (T_4 - T_6)$	

h = ———

$T_4 = \underline{150 + 32} = 91^oC$

2

$$Nu = \frac{h_c L}{K_a} = \left[0.060 - 0.17\left(\frac{S}{90^0}\right)\sigma r\right]^{1/3}$$

$$\frac{h_c L}{K_a} = \left[0.06 - 0.17\left(\frac{S}{90^0}\right)\right]\left[\frac{g\theta\rho_a^2 L^3}{\mu_a^2 T}\right]^{1/3}$$

$$h_c = k_a\left[0.060 - 0.17\left(\frac{S}{90^0}\right)\right]\left[\frac{2g\left(T_B - T_g\right)\rho_a^2}{\mu_a^2\left(T_a + T_g\right)}\right]^{1}$$

$h_c = 0.31766461 kW/m^2$
Therefore:

$q_{46\ cond} = 3.176646 \times 10^{-1} \times \pi \times 25.4 \times 10^{-4}$

$\times (91 - 36) = 1.3722122564$ kW

$q`'_{46\ rad} = \sigma D_4 \pi \alpha_5 (T_4 - T_7)$

$= 25.4 \times 10^{-3} \times 5.6704 \times 10^{-4} \times \pi \times 0.9 (91 -$

36)

$= 2.204449364 \text{ X } 10^{-3}$Kw

	TOTAL CONCENTRATOR HEAT LOAD $q`'_{total\ (conc)} = q`'_{23\ cond} + q`'_{12conv} + q`'_{3\ sol,abs}$ $+ q_{radcond\ brack} = 0.71664 \times 3 + 2\{1.37221$ $+ 2.204493 \times 10^{-3}\}_{-} = 5.16382922kW$	
	AREA OF SOLAR COLLECTOR $= \frac{\text{Design collector load}}{\text{Mean solar irradiation absorbed/area}}$ $= \frac{34.563133 + 5.16382922}{280.4}$ or L = 2B Length of concentrator = 0.*8*29418211m Width of concentrator = 0.2147091055m	or L = 2B Length of concentrator = 0.*8*29418211m Width of concentrator = 0.2147091055m

	REQUIRED AMOUNT OF ZEOLITE $V = \pi r^2 L = \pi(25.4 \times 10^{-3})^2(8.294) =$ $0.016810527 m^3$ $M = \rho V = 0.8 \times 10^3 \times 0.016810527 =$ 1.3448kg But considering for 500g of Zeolite give dimensions of the collector to be 600mm by 450mm which includes a 10% factor of safety. $= \frac{500 \times 10}{0.8 \times 10}$ $= 6.25 \times 10 \quad 1$	Length of concentrator = 0.829418211m Width of concentrator = 0.2147091055m

Properties of Zeolite Mass of Zeolite = 500g = 0.5kg Density of Zeolite = 0.8kg/dm^3	LENGTH OF ABSORBER PIPE Volume of a cylinder = $\pi r^2 L$ = = 6.25×10^{-4} = (L = 3/4 full) = $\pi (25.4 \times 10^{-3})^2$ 0.631490567m For Length of absorber pipe = 0.631490567m Let width=3/4 of length pipe = 0.4672m a 15% factor of safety	

From thermodynamic tables for water and steam we obtain that for T=2^{o}C $P_{sat@2oC}$ = 0.007054

For t= 0^{o}C

$Ps_{at@0oC}$

= 0.006112

Also at this condition

Assuming we have pure water in the suction line, then the specific volume Vs=0.10001x 10^{-2}

Therefore

PIPE LINE SIZING

SUCTION LINE

For the Suction line also it should be sized such that the pressure drop will give a maximum temperature drop of 1^{o}F per 100ft of 0.555^{o}C per 30.46m run if pipe.

$\Delta t = 2^{o}C \quad \Delta P_{sat} = 9.42x10^{-4}$

But $\Delta t = 0.555^{o}C$,

$$\frac{9.42 \times 10 \quad \times 0.555}{2}$$

$$\left(\frac{\Delta}{\quad}\right) \leq \frac{9.42 \times 10 \quad \times 0.555}{2}$$

$$\left(\frac{\Delta}{\quad}\right) \leq 0.85819$$

$$\dot{} = (h \quad - h \;)$$

$$\dot{} = \frac{\dot{}}{(h \quad - h \;)} = \frac{34.563133}{29.57 - 21}$$

$$= 4.033$$

$4.033 \times 0.10001 \times 10^{-2} = 4.0334x10^{-3}$

$$\dot{} = \frac{}{4}$$

$$= \frac{4\dot{}}{}$$

volume flow rate $\dot{} = m_s V_s$ Assuming that for the pipe flow the Euler equation holds since density changes can be considered small Neglecting the kinetic and potential energy terms as they will be small which implies	$h = \frac{\Delta}{} + \frac{\Delta(\ )}{2} + \Delta$ $= \frac{\Delta}{}$ Applying also the Darcy- Weisbach formula to obtain pressure drop in the pipe we have $h = \frac{}{2}$ Where f_s is the friction factor and L is the pipe length. Combining equations we have $(\frac{\Delta}{}) = \frac{}{2}$ Noting $(\frac{\Delta}{}) \leq 0.85819 \quad /$ $\frac{}{2} \ \frac{4}{} \leq 0.85819 \quad /$ $= \frac{16}{2 \times 0.85819 \times}$ $\geq 4.98318 \simeq -in$	$= -in$

DISCHARGE LINE

For the discharge line also it should be sized such that the pressure drop will give a maximum temperature drop of 1^oF per 100ft of 0.555^oC per 30.46m run if pipe.

$\Delta t=2^oC \quad \Delta P_s=4.304x10^{-3}$

For $\Delta t=0.555^oC$

$$\Delta \quad = \frac{4.304 \times 10 \quad \times 0.555}{2}$$

Therefore the desired pressure drop per unit length of piping is

$$\left(\frac{\Delta P}{L}\right) \quad \leq \frac{1.19436 \times 10 \quad \times 10}{30.46}$$

$$\left(\frac{\Delta P}{L}\right) \quad \leq 3.921077 \text{Nm}$$

Similarly,

$$d \quad \geq \frac{16\dot{V} \quad \rho \quad f}{2 \times 3.921 \times \pi}$$

$$= \frac{1}{} = \frac{1}{0.10044 \times 10} = 995.62$$

$$= \frac{1}{} = \frac{1}{0.10001 \times 10} = 999.90$$

$$— = 0.219811753$$

$$d \quad = 3.68060354\text{mm} \approx \frac{1}{8}\text{in}$$

CHAPTER FOUR

CONSTRUCTION, TESTING AND RESULTS

4.0 INTRODUCTION

The solar refrigerator designed and constructed is extremely simple; the local industries are capable of producing it. It is a simplified model and improved type of the conventional flat plate powered solar adsorption refrigerators developed over the years. The refrigerator has no moving any parts, water is used as the working fluid and highly porous Zeolite is used as the adsorber.

4.1 CONSTRUCTION

Construction processes involves the cutting and forming of the designed components to the specified shape and dimension. These design specification give particular and qualitative information about the system to be fabricated, puts certain factors into consideration for effectiveness and ease in the construction process.

In the course of this work a lot of literature was reviewed which was the guide in showing what pitfall to avoid.

The factors considered in the construction of the parabolic trough solar collector included stability, and accuracy of the parabolic trough profile, optical error, tolerance, method of fabrication, cost, and material availability.

Here the design's objectives were not linked to maximizing thermal efficiency, but also for cheaper, labour intensive, and production techniques.

The development of the solar adsorption refrigerator began with the production of the adsorbent (Zeolite) which was immediately followed by the construction. Production processes are fully discussed is subsequent Table 4.1 below.

The refrigerator is constructed from locally available materials and consists of the following parts:

i. A parabolic trough concentrator; which is used to collect the solar radiator and concentrate it on the absorber placed at its focal point.
ii. A copper pipe painted black, which is the absorber and contains the Zeolite + water pair
iii. An attached heat exchanger made of iron tubing (condenser) which cools the desorbed water vapour into liquid state.
iv. An accumulator which stores the condensed vapour before it enters the evaporator.
v. An insulated cooler box (refrigerator).
vi. Evaporator.
vii. Control valves
viii. Transport pipes
ix. Zeolite
x. Distilled water

4.2 METHODOLOGY

The development of the solar adsorption refrigerator began with the production of the adsorbent (Zeolite) which was immediately followed by the construction. Production processes are fully discussed in subsequent sections below.

4.3 PRODUCTION OF ZEOLITE A

The beneficiation of the Kankara kaolin (a clay sourced from a village in Katsina State, Nigeria) was done in a manner similar to that reported by Aderemi, B.O., (2004).and Oriuwa Lazarus Jan (2002). Clay generally is unreactive in the natural form. Subsequently, it was transformed to a more reactive(amorphous) form by subjecting it to heating at 600 ^{0}C before using it as a reactant. Dealumination of metakaolin was affected by leaching out the structural alumina with sulphuric acid, to meet the silica–alumina mole ratio required for the targeted Zeolite.

A gel from the dealuminated metakaolin and a solution of sodium hydroxide was prepared based on the recipe required for the synthesis of Zeolite A. After this the gel was left to age for 3 days at room temperature in a polypropylene container. The gel sample was heated in an autoclave (WS2-84-64, model- 7101) set at 100^{0}C, for 16 hours. The post synthesis treatment involved washing off the excess sodium hydroxide from the synthesised Zeolite and drying at 150^{0}C, for 3 hours. The dried sample was later calcined at 300^{0}C.The analyses carried out on the synthesized samples include; x-ray diffractometry (Siemens, D500) as described by Oriuwa(2002).fig 4.1 shows a picture of the produced Zeolite A while appendix B shows the sample calculation for the mix



Fig 4.1 produced Zeolite A

4.4 **COLLECTOR STRUCTURE FABRICATION**

Factors considered in the construction of the parabolic trough solar collector included stability and accuracy of the parabolic profile, optical error tolerance, method of fabrication, cost, material availability and strength constraints.

Brooks M. et al. (23) proposed a parabolic trough design approach for developing nations, where design objectives are not limited to maximizing thermal efficiency but must also favour cheaper, labour intensive design and production techniques.

Like many developing countries, Nigeria exhibits less advanced manufacturing capabilities. The construction of the collector reflected this. A flat bar section structure was chosen as it represented an achievable solution in terms of accessibility, accuracy, ease of fabrication and cost. The collector has a length of 0.6 m, aperture width of 0.45 m and a rim angle of 77.5°.Four lightweight parabolic ribs were cut from 25 mm thick flat bar section using basic workshop tools. These were curved in the shape of the parabola in the shape of the rim angle. Similar flat-bar sections provided additional

bracing in a perpendicular direction. The accuracy of the parabolic ribs and the method of assembly reduced the time and cost of fabrication and minimised the degree of technical skill required by workshop staff, while providing sufficient structural strength. The sheet of galvanized iron is then placed in the formed on the parabolic ribs. Strips of plane glass mirror of dimension 600 X 25mm are aligned and placed on the galvanized iron sheet, which was welded onto the profile formed by the parabolic ribs

CONSTRUCTION PROCESSES

S/No.	**Component**	**Material**	**Process Description**	**Equipment Used**
1	Parabolic trough Concentrator	1/2" Flat bar section Galvanised Iron sheet Strips of plane mirror	Marking and cutting of the G.I Sheet to rectangular shape of dimension 600mmX450mm Rolling of G.I sheet to form parabola. Parabola rib frame produced by cutting the flat bar section, rolling it to form parabolic shape by setting it to the	Scribe Compass Welding machine Rolling machine Hacksaw Scissor

			design rim angle $\psi=77.5^{o}$and welding it to maintain that position	
2	Absorber	Copper(ϕ25mm)	This is constructed by cutting the copper pipe to the required length and threading it on one end. The opposite end is completely sealed by brazing. A black coating was applied to both absorber tubes to reduce emittance and increase absorptance. Two holes of diameter 6.25mm are then drilled on one side to form the outlet and inlet vent by a	Measuring tape Hack saw Drill Brazing machine Die Vice

			ϕ6.25mm extrusion pipe	
3	Condenser	4000mm, One quater inch copper pipe	Copper pipe is formed into the condenser S- shape by a copper bending it carefully to the required radius for each curve.	Measuring rule Small hack saw Copper bender
4	Accumulator	steel	An existing accumulator was resized by cutting and welding it to suit the design	Vice Hack saw Measuring tape Welding machine
5	Cooling Box	Galvanised iron sheet Aluminium sheet fibre	The outer casing is Produced from galvanised iron sheet and the cooling chamber is produced from	Marking tools Scissors Welding machine

			aluminium sheet. They are both marked to specified dimensions as shown on the design drawings. They are then formed into the box shape, welded and placed in each other being separated by fibre insulation.	
6	Evaporator	Copper Aluminium	It is produced by cutting one quarter inch copper pipe into length and rolling into the desired S shape. It is then placed on side on the of the aluminium box on the inner side of the outer casing and	

			soldered to it. This assembly is then placed in the outer casing.	
7	Parabolic trough Support	1" flat bar section	Cut to the design length as shown in detail drawing No.7it is then slightly bent to provide a firm support for the parabola trough.	Hack saw Drill File
8	Refrigerator stand	1" angle iron section	Section is cut and welded in the shape required which is to provide for strength and rigidity	Hack saw Drill File

4.6 ASSEMBLY

Assembly of the solar refrigerator is the fitting together of the components or produced parts to make the finished product.

4.6.1 parabolic trough concentrator

The parabolic trough is formed by bending the 4 flat bar sections to suit the rim angle of 77.5^{o} and placing the equidistance along the 600mm length. Then 3 additional flat bar section are the laid perpendicularly across the four sections to provide rigidity by welding. The galvanised iron sheet is then laid directly on the parabolic ribs cage to provide for a surface to attach the mirror strips. A layer of insulation is then placed between the G.I Sheet ant the linearly aligned mirrors as can be seen it Fig 4.2



Fig 4.2 showing the parabolic trough concentrator

4.6.2 The absorber

The absorber was constructed by cutting a 25mm copper pipe to a length of 600mm. One end was completely sealed by brazing and threading the opposite side.

The absorber was opened and loaded with the wetted Zeolite and tightly screwed. The parabolic trough and absorber were mounted onto the stand and fastened there via 13mm bolts. The absorber was placed at the focal length of the parabola and held there by a support fastened also to the assembly. The condenser was next attached on the stand via 13 bolts. The cooling box was the position on the assembly as shown in fig 4.

Below. The system connection was completed by putting on the service pipes and control valves as seen in fig 4.3 below



Fig 4.3 Assembled adsorption refrigerator

4.7 TESTING OF THE SOLAR REFRIGERATOR

A test on the constructed refrigerator was conducted to ascertain the functionability of the system. The first test was carried out for a period of five days in the month of January 2008 , a month with the lowest solar irradiation and the second test carried out in May 2008. Temperatures of the absorber, condenser, evaporator, and the ambient were monitored. A thermocouple is set-up to monitor the temperatures of the key components of the system, while the ambient temperature is noted by a normal clinical

thermometer. The collector is placed in the east west direction for maximum solar collection. The test set-up is shown in fig 4.4 below



Fig 4.4 Testing Set-Up

Starting procedure:

300g of any adsorbent power was generated manually by soaking it into 280g of distilled water of equivalent volume 0.28 m^2 . the resulting paste was weighed and found to be 580g and is manually loaded in it the copper pipe of diameter 25mm which is screwed open on one end ,while in the absorber and the inlet and outlet valves are completely closed. The absorber is longitudinally placed at the focal plane of the concentrator located 11cm from the base of the parabola profile. The valves are kept closed for 8AM to 2PM, and between this period the required regeneration temperature is attained and forces water vapour to desorb at constant pressure hence building up a pressure (partial) in the vacuum. The experimental cycle conforms to the proposed adsorption cycle of the solar refrigerator working without a pump considered for the design fig 3.1. In the beginning, the Zeolite is saturated with water which is

approximately 93% by weight. The solar absorber is heated up by the solar radiation, aided by the concentrator which transfers heat to the packed Zeolite.

By noon the maximum temperature is attained and desorption of the water vapour takes place. The outlet valve is then opened and the vapour escapes to the air cooled condenser and cools at ambient temperature. The water vapour is condensed and is collected in the accumulator at the bottom of the condenser attached to the frame of the concentrator. At t=8 the closed outlet valve is opened and the refrigeration process is started and by gravity the water flows through a tube into the evaporator.

4.8 RESULTS

Two sets of test were carried out at different times and seasons of the year. The first test was carried out in January 2008 a month with very low solar irradiance and the second test was carried out in May 2008.

. The temperatures at different places in the system i.e. cold chamber, evaporator, adsorber, ambient. Were taken simultaneously with the same instrument. The results of the cooling experiments are shown in the tables and figures below

Table 4.1 Temperature readings 14th Jan2008

Time(Hrs)	Ambient temp^{o}C	Absorber Temp ^{o}C	condenser Temp^{o}C	Evaporator Temp ^{o}C
8:00	17	17.5	17	18
9:00	18	19.7	18	18.5
10:00	20	20.8	20	20
11:00	24	21	24	31.5
12:00	25	31	25	35.4
13:00	28.5	41.6	28.5	28.4
14:00	29	43.5	29	28
15:00	28	52.9	28	28
16:00	26	51	26	27.8

Table4.2 Temperature readings 15th Jan2008

Time(Hrs)	Ambient temp^{o}C	Absorber Temp ^{o}C	condenser Temp^{o}C	Evaporator Temp ^{o}C
8:00	18	19.5	18	18
9:00	18.5	20.8	18.5	18.5
10:00	20.5	29.8	20.5	20
11:00	24	43.1	24	31.5
12:00	25	50.4	25	35.4
13:00	26.5	54.7	26.5	28.4
14:00	29	55.2	29	28
15:00	29	54.6	29	28
16:00	28	52.8	28	27.8

Table 4.3 Temperature readings 16th Jan2008

Time(Hrs)	Ambient temp^{o}C	Absorber Temp ^{o}C	condenser Temp^{o}C	Evaporator Temp ^{o}C
8:00	17	12.5	17	17
9:00	18	18.5	18	17.7
10:00	20.5	27.2	20.5	26
11:00	20.5	33.8	20.5	26
12:00	27.5	37.9	27.5	26.4
13:00	28	56.2	28	26
14:00	30.5	52.5	30.5	26
15:00	30	45.5	30	25.5
16:00	29.5	45.3	29.5	25.5

Table 4.4 readings 17th Jan 2008

Time(Hrs)	Ambient Temp^{o}C	Absorber Temp ^{o}C	condenser Temp^{o}C	Evaporator Temp ^{o}C
8:00	17.5	16	17	24
9:00	19	17	21.9	24
10:00	19.5	33.7	39.9	24
11:00	20	35.1	45	24.4
12:00	20.5	39.1	52.4	24
13:00	27.5	34.7	51.4	24
14:00	27.5	57.4	55.4	24
15:00	27.5	39.6	33.4	24
16:00	25	37	30	24

Table 4.5 Temperature readings 18th Jan 2008

Time(Hrs)	Ambient temp^{o}C	Absorber Temp ^{o}C	condenser Temp^{o}C	Evaporator Temp ^{o}C
8:00	17.5	11.9	17	18
9:00	18	12.7	19	18.5
10:00	20.5	32.4	38.6	20
11:00	24.5	39.7	50.2	31.5
12:00	25	39.1	53.3	35.4
13:00	27.5	34.7	51.4	28.4
14:00	28	34.5	47.9	28
15:00	28	35.4	47.8	28
16:00	27	33	39	27.8

Table 4.6 Temperature readings 6th May 2008

Time(Hrs)	Ambient temp(^{o}C)	Absorber Temp(^{o}C)	condenser Temp(^{o}C)	Evaporator Temp (^{o}C)
8:00	27	27	27	27
9:00	29	32	29	27
10:00	30	51.9	33	28.9
11:00	30	55.8	36.1	29.3
12:00	33	56	36.4	29.9
13:00	34	58.9	39	30.8
14:00	35	48.9	37.8	32
15:00	33	44.7	36.2	32
16:00	33	40	36	32

Table 4.7 Temperature readings 7th May 2008

Time(Hrs)	Ambient temp^{o}C	Absorber Temp ^{o}C	condenser Temp^{o}C	Evaporator Temp ^{o}C
8:00	28	31	28	11.5
9:00	29	41.6	29	11.4
10:00	30	43.5	30	13
11:00	30	51	30	13.7
12:00	32	52.9	32	14
13:00	34	60.1	34	14
14:00	33	55.2	33	15
15:00	31	54.6	31	16.5
16:00	30	52.8	30	16

Table 4.8 Temperature readings 8th May 2008

Time(Hrs)	Ambient temp^{o}C	Absorber Temp ^{o}C	condenser Temp^{o}C	Evaporator Temp ^{o}C
8:00	28	25	27	9.8
9:00	29.5	41.6	29	10.6
10:00	30	43.5	30	10.6
11:00	31	51	31	11
12:00	33	52.9	33	11.9
13:00	35	55.2	34	14.7
14:00	34	54.7	34	15.2
15:00	33	52.8	32	16
16:00	33	50.4	31	16.3

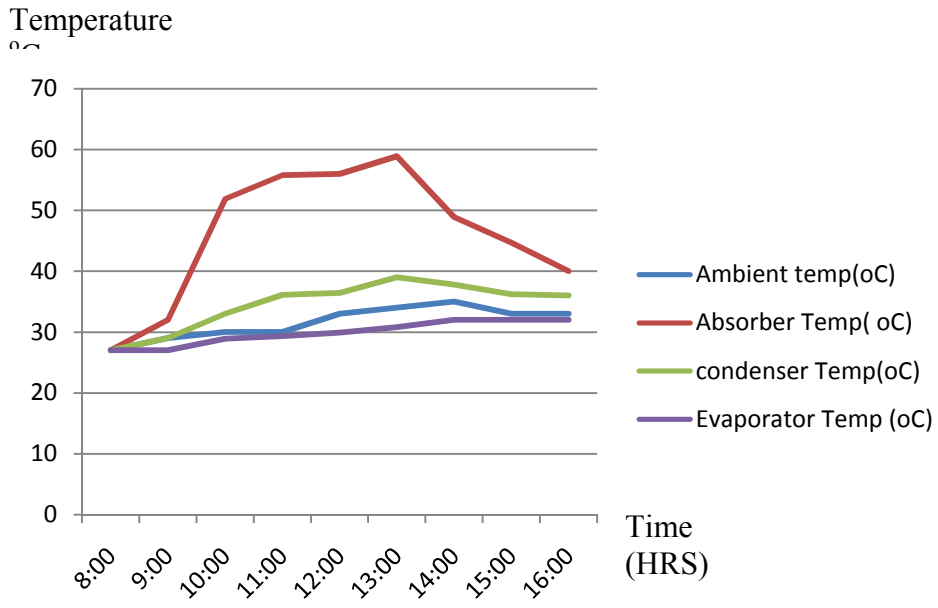


Fig 4.5 temperature profile for 6th may 2008

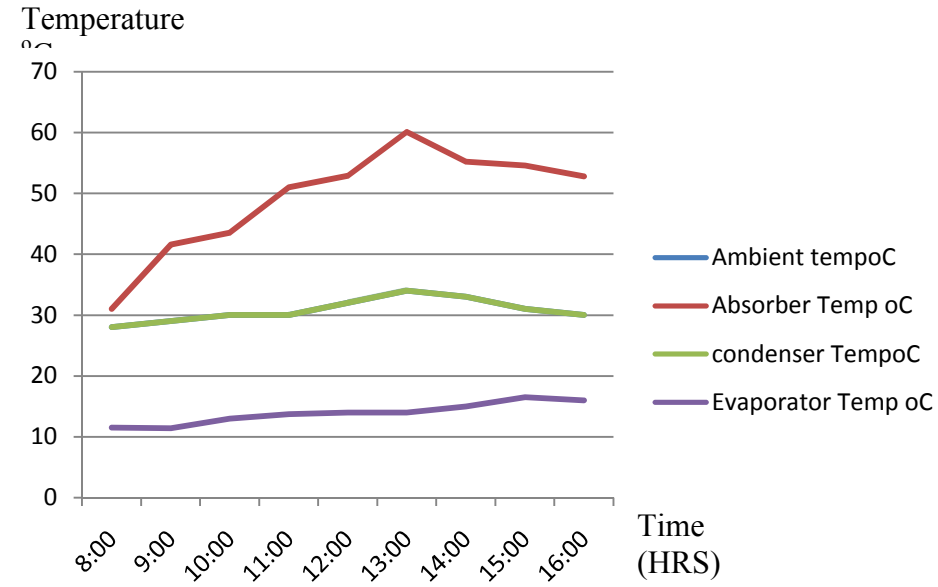


Fig 4.6 temperature profile for 7th may 2008

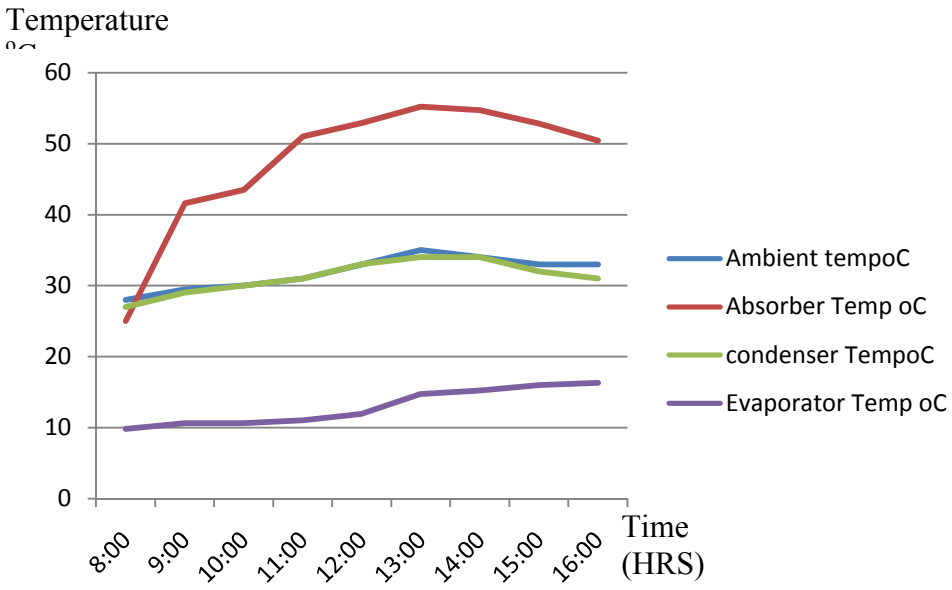


Fig 4.7 temperature profile for 8th may 2008

The produced Zeolite A was also subjected to different tests to characterize it and obtain the thermal stability.

Tests carried out included X-ray diffraction, TGA/DTA. Some results of the characterization are seenn in table 4.6 below for Zeolite A. Appendix C contains results for Kaolin and metakaolin

Table 4.6shows some determined properties of the produced Zeolite A

Zeolite	Water Adsorptivity	Pore size (A^o)	Ion exchange capacity	composition		Sorption capacity wt%		
				Si/Al	cation			
A	70%	4		1	Na	23	13	1

4.9 DISCUSSION

The refrigerator was tested according to the procedure outline by Siegfried et.al. Temperatures of various parts of the system was taken simultaneously and recorded hourly.

The testing was done in two different times of the year. The first test was done in January a month with one of the lowest solar irradiation of average intensity of 5.66 KW/m/d (20.38 MJ/m/d) while the second was done in May with a relatively higher isolation of 6.41KW/m/d (23.08MJ/m/d).

Typical results obtained are shown in the tables below. Tables 4.1 to 4.5 show results for the test taken in Jan 2008 .the temperature profile shows that the maximum temperature achieved on the absorber was 56.2 ^{o}C and a minimum of 11.9^{o}C. The evaporator temperature recorded a minimum temperature of 18^{o}C and a maximum temperature of 35.4^{o}C. No cooling effect was however noticed in the cooling box over the five days tested in January due to the time of the year testing was carried out and in perfections in the fabrication process. Table 4.1, 4.2, 4.3, 4.4 and 4.5 shows the relationships of the temperature with the time of the day tests were carried out. The temperatures from the evaporator reveal the loss of heat from the cooling box as it had almost the same values as the condenser. Cooling was however seen to occur on the absorber it self on the two days which recorded the highest absorber temperature indicating the desorption process had occurred.

The second tests were conducted in May 2008 with a few corrections on parts of the system where sources of error were noticed to have occurred. Surface of the cooling box was taken off and increased with insulation where the outer casing overlapped the

evaporator. Transport pipes were changed to eliminate the number of joints in the flow line. These slight modifications gave slight improvements to the results obtained from the system.

Test was set-up on the sixth of May with the absorber, evaporator, and condenser at the same starting temperature. During experiments, some temperatures were nearly constant. Cooling effect was noticed on the second test day with the evaporator at 11^{o}C and gradually increased to 16^{o}C at the end of the day as seen in table 4.7. Maximum absorber temperature attained over the testing period was 58.9^{o}C. The third day of testing showed a marked increase in cooling as the evaporator temperature dropped to 9.8^{o}C recorded in table 4.8.

The cooling is seen to be intermittent as described by the refrigeration cycle. The cooling effect is pronounced in the early hours of the morning and linearly increase with the time of the day as shown in figures 4.8, 4.9.and 4.10. This indicates a short come in the cooling box fabrication.

Absorber temperatures rise to a peak value between 1p.m and 2 p. m as is shown in figure 4.5 to 4.7. The degree of refrigeration higher cooling power is achieved with desorption temperatures greater than 120^{o}Ctempretuer of the condenser and ambient appeared to be fairly constant during the experiment as the condenser is air cooled. The parabolic trough /absorber pipe ratio is a considerable factor in the low absorber temperature attained and a resulting low adsorption/desorption rate

Miguel et.al (2003) fig 4.8 shows the drying curve for Zeolite A obtained at atmospheric pressures with samples of Zeolite put at different temperatures in an electric oven

From the curves he concluded that it is not recommendable to reduce the humidity from its initial 30-35 %(dry bases) at saturation to below 5%.

Further drying would result only in a small improvement of the capacity of the Zeolite to adsorb water, but at the expense of a big amount of additional energy and time required.

It can also be seen that 250^{o}C is an appropriate regeneration temperature. At this temperature one gets in 2.5hours Zeolite with 5% humidity (with 84% of the water extracted). At 200^{o}C one would need 6hours to reduce humidity to 10 %(extracting 66% of the water).

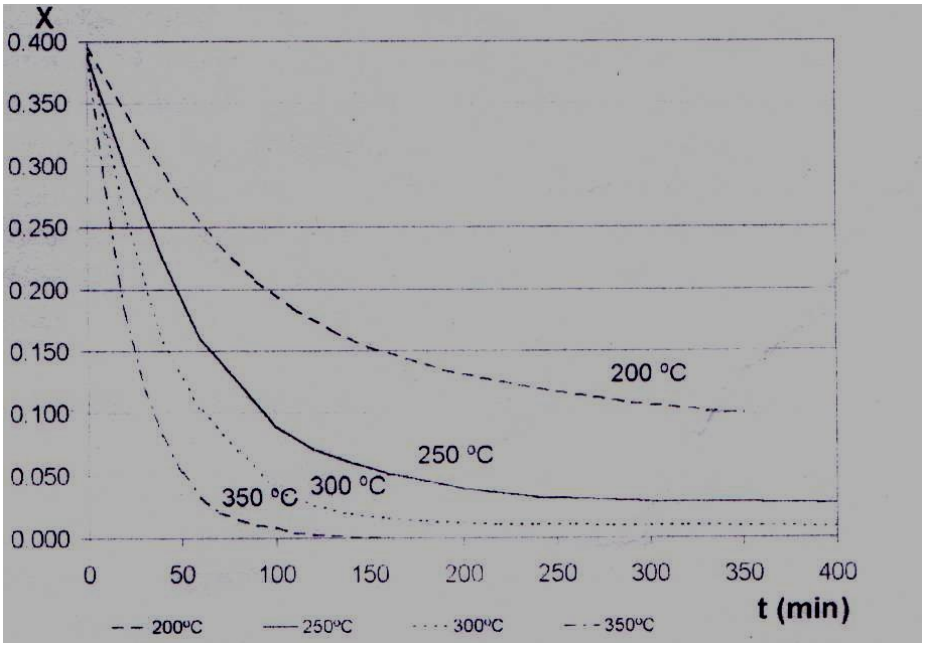


Fig 4.8 Desorption curves for Zeolite A

Thermogravimetric analysis (TGA) is an analytical technique used to determine a material's thermal stability and its fraction of volatile components by monitoring the weight change that occurs as a specimen is heated. In DTA one instead measures the

temperature difference between an inert reference and the sample as a function of temperature. When the sample undergoes a physical or chemical change the temperature increase differs between the inert reference and the sample, and a peak or a dip is detected in the DTA signal

The thermal properties of few natural Zeolite have been studied and investigated by DTA, and TGA,. This combination of techniques facilitated a better description of the dehydration phenomena and the mass of the sample as a function of temperature.

From the DTA/TGA, samples were compared for the kaolin, Metakaolin and the Zeolite as can be seen in appendix C.

DTA, and TGA, were performed according to the methods described earlier (van Reeuwijk, 1971) in a laboratory in Oman .a heating rate of l0'C/min. was used for DTA and TGA A representative specimen of the kaolin, metakaolin and Zeolite tested to illustrate the characteristic properties

The DTA and TGA results and curves are a plot of weight loss against temperature and are presented in tables 4. 11, 4.12 and 4.13 in Appendix C respectively

The DTA and TGA traces of Kaolin, metakaolin and Zeolite A shows, Dehydration occurs, with temperature, Fig 4.9; appendix C shows the weight loss as a function of temperature. This is shown as a weight loss percent of the total weight. The loss of water from kaolin was gradual over the temperature range 40^{o}C to about 180^{o}C which becomes constant over the temperature range of 200^{o}C to 500^{o}C and a pronounced drop in weight at 550^{o}C to 600^{o}C. From this temperature the loss of water becomes constant. The kaolin sample becomes thermally stable at 800^{o}C

The metakaolin stage is seen in appendix C fig 4.10 there is a gradual loss of water over the temperature range. The water loss abrupt at 970^{o}C where there is no loss in weight with increase in temperature.

The Zeolite TGA/DTA is seen in fig 4.11 (appendix C). the loss of water is gradual over the temperature range of 40^{o}C to about 500^{o}C and becomes constant at 550^{o}C over the temperature range. The Zeolite was found to be thermally stable at 600^{o}C and the regenerative temperature is also seen from graph to be over 200^{o}C. The desorption of water from Zeolite is seen to be greater for the Zeolite followed by the metakolin and lastly the kaolin due to the pore sizes as the facilitated by the substitution of the Si-Al atoms in the parent material and alteration in the physical and chemical properties as can be seen in tables 4.11 through 4.13, appendix C. The DTA instead measures the temperature difference between an inert reference and the sample as a function of temperature. DTA detects the release or absorption of heat, which is associated with chemical and physical changes in materials as they are heated or cooled. Such information is essential for understanding thermal properties of materials. Analysis of decomposition of glass batch materials, crystalline phase changes, chemical reactions and glass transition temperature are some of the properties measured with DTA. The temperature range of the instrument is from ambient to 1000º C.

4.10 COST OF PRODUCTION OF THE REFRIGERATOR

The production of this refrigerator consists of two parts as shown in the tables below: first the production of the adsorbent (Zeolite) and then the fabrication of the refrigerator

Table 4.8: Cost of Zeolite production

MATERIALS	PROCESS	QUANTITY	UNIT COST(₦)	TOTAL COST(₦)
Kaolin	Dealumination	1Kg	500/50 grams	10000
Metakaolin Distilled water Sodium hydroxide Kerosene Furnace	Beneficiation Calcination	1 litre 2 bottles 1 gallon	50 550 400 3000	50 1100 400 2000
	Labour		300	2000
			TOTAL	**₦ 12050**

Table 4.9: Solar refrigerators materials and cost

QUANTITY	MATERIAL	COST
1 sheet	Galvanized Iron(G.I)	₦ 5500
1	1”Angle iron	₦ 1100
1	Flat bar	₦ 600
	Fibre	-
1	Aluminium	₦ 1780/Sq m
1 roll	–Copper pipe	₦ 2000
1	Plane mirror	₦ 340
1	1” copper pipe	₦ 1500
4	Bolts& nuts	₦ 100
	Paint & tinner	₦ 100
	Workmanship	₦ 3000
	Total	₦ 16020

Grand total = ₦ 28,070.00

CHAPTER FIVE

SUMMARYCONCLUSION AND RECOMMENDATIONS

5.0 SUMMARY

A solar adsorption refrigerator using Zeolite as the adsorber and water as the working fluid was designed, fabricated, and tested. The system consists of a parabolic trough concentrator, an absorber, a condenser, an accumulator, evaporator and a cooling box. The system was subjected to two tests, the first was carried out in January 2008 and the second was done in May 2008. The first test fell short of expectation due to imperfections in the construction and the time of the year testing was carried out. Lowest collector temperature was 11.9^{o}C and the highest was 57.2^{o}C which indicated we fell way below the desorption temperature for Zeolite A the lowest evaporator temperature recorded was 18^{o}C. With slight corrections in the Refrigerator the second test yielded better results. An evaporator temperature as low as 9^{o}C was recorded on one of the test days. A refrigerator of this sort when fully developed; based on this concept and technology will offer desirable advantages such as:

a. Light weight and relatively low cost
b. Non- toxic operation
c. Independence from the electrical grid

Several of the disadvantages of the adsorption refrigerator have become obstacles for popularity for domestic use.

a. Long adsorption /desorption time
b. Small refrigeration capacity per unit mass of the adsorbant

c. Low COP values

The overall cost of the model built cost about ₦ 28,070.00

5.1 CONCLUSION

The objective of this research which was to design ,construct and test a solar adsorption refrigerator using Zeolite as the adsorber and water as a refrigerant, with locally available materials was achieved.

It has been shown that refrigeration effect can be produced by a very simple adsorption cycle using locally produced Zeolite as adsorbent and water as the refrigerant in such a simply designed solar adsorption refrigerator as presented in this work.

Theoretically a solar irradiation of 300W/m^2 is sufficient to reach the required desorption temperature in the range of 150^{o}C-170^{o}Cwhich is attainable in the main solar testing period in Zaria. Total pressures in the system may increase due to leakages in piping network or desorption of air from inner surfaces. This effect can reduce the adsorption rate and boiling temperatures of the refrigerant. The efficiency of the whole system depends on the efficiency of the solar collector and the system operates on an intermittent water-Zeolite adsorption cycle which is capable refrigeration for food conservation in rural areas where no electricity is available.

In conclusion it can be said that, using Zeolite as an adsorber, a heating temperature of less than 100^{o}C is too low to desorb water over a short period which implies very slight refrigeration effect would be experienced, whereas temperatures higher than 200^{o}C does not necessarily increase the cooling power anymore. This solar powered adsorption

refrigerator has a good advantage in energy conservation and sustainable development. However the refrigerator has some short comings that still have to be resolved:

5.2 RECOMMEMDATIONS

a. Advanced manufacture of the parabola trough collector to meet specifications of the rim angle and a perfect curve should be used to provide a perfect profile
b. A tracking system to improve the collector efficiency
c. Automatic control valves to automate each cycle should be employed to eliminate the manual opening and closing of the valves which might poise very difficult to fulfil by the rural users for where the refrigerator is thought for.
d. Ensure the geometry of the used absorber vessel does facilitate homogenous adsorption and desorption processes.
e. Extensive research should be carried out on the Zeolite to find out ways lower the high regenerative temperature.
f. More efficient welding and soldering techniques for piping should be sought to improve the system by making it devoid of air vaacums.

   Based on these findings, modifications of the refrigerator, based on the same intermittent water-Zeolite adsorption cycle are to be considered in this line with these technical issues.
g. Establish an appropriate collector/ absorber ratio

REFERENCES

Activated alumina & molecular sieves axens http.www.axens. Net.

Aderemi B.O (2004) Preliminary studies on synthesis of Zeolite from local clay. Nigeria journal of scientific research 4(2) :7-12

Alghoul, M.A. Sulaiman M. Y., Azmi, B.Z. and Abdul.Wahab, M. (2007). Advances on multipurpose solar adsorption systems for domestic refrigeration and water heating. Applied Thermal Engineering Journal, ISSN: 1359-4311, 27 (5-6), pp. 813-822

Andreas E. S, Warecks G, Derewinski and M. Lercher J. A. (1989) Adsorption of water on ZSM5 Zeolites American Chemical society Journal Phys. Chem pp 4837-4843

Anyanwu E. E , 2004 May: Review of solid adsorption solar refrigeration II: An overview of the principles and theory Energy Conversion and Management Volume 45, Issues 7-8 , Pages 1279-1295

Anyanwu E. E.and Ogueke N. V.(2004) Thermodynamic design procedure for solid adsorption solar refrigerator Renewable Energy Volume 30, Issue Pages 81-96 Elsevier Ltd

ASHRAE Handbook, Refrigeration Fundamentals. SI Edition. (1985)Published by the American Society of Heating, Refrigerating and Air Conditioning Engineers, Inc. 1791 Tullie circle N,E. Atlanta, GA30329, Ed. Frank Kreith Boca Raton: CRC Press LLC,

Attah A.Y., Ajayi, O.A, and Adefila S.S (2007) Synthesis of faujusite Zeolite from kankara clay. Journal of Applied sciences research. Insinet publication

Awoniyi J.A: (1980). The design and construction of solar powered vapor absorption refrigeration system. M.Sc project Department of Mechanical Engineering , Ahmadu Bello University Zaria

Bala E. J. (1980). Solar energy collector design or rural refrigeration M.Sc project Department of Mechanical Engineering, Ahmadu Bello University Zaria

Brooks M and Harms T (1994). Design, construction and testing of parabolic trough solar concentrators for developing countries. Energy conversion management vol 35 No.7, pp. 569-573

Chaouachi B. and Gabsi S. (2007). Design and Simulation of an Absorption Diffusion Solar Refrigeration Unit American Journal of Applied Sciences 4 (2): 85-88, 2007

Chunfang T., Qinghai L, Xiangmei L, and Xiaojuan Z. (2006) Comparison of Several Eco-friendly Refrigeration Technologies. China Renewable Energy Resources and a Greener Future ,Vol.VIII-4-6

Critoph,R.E. (1988). Limitations of adsorption cycles for solar cooling. Solar Energy, 41(1), 23- 31.

Critoph R.E. (1999) Rapid cycling solar/biomass powered adsorption refrigerant system Renewable energy 16 pg 673-678

Concentrating solar power: March 2001Energy from mirror: Journal energy efficiency and renewable energy.

Duffie J. A., and. Beckman W. A, (1974) Solar Energy Thermal Processes, Wiley, New York,.

Forristall R. .(2003) Heat transfer analysis and modelling of a parabolic trough solar receiver implement in engineering Equation solver . Technical report national renewable energy laboratory

Fundamentals of Zeolite/water Technology (2007) pp1-2. http//www.zeo-tech-de/htm/e/e-grund/.htm..

Hellene M. Simonot .G (1979). Thermodynamic and structural features of water sorption in Zeolites clays and clay minerals, vol. 27, no. 6, 423428,.

Hildbrand C., Dird P., Pous M, and Bucther F (2004). New solar powered Adsorption refrigeration with high performance Solar Energy, 77, pp. 311-318.

Ing. Eduardo D. Sagredo PE (2004) Design and construction of solar energy refrigeration using vacuum concentric tubes with adsorption severed LACCEI

international Latin America and carrebian conference for engineering and Technology (LACCEI 2004)

Jordan R. C, Gayle B. P (1962). Refrigeration and air Conditioning, prentice Hall Inc Englewood cliffs.

Joa˜o Pires and M. Brotas de Carvalho Water adsorption in aluminium pillared clays and zeolites www. Google.com

Mannan R.D., Bannerot R.B: (1978). Optimal geometries for one and 2 faced symmetrical side wall booster mirrors: solar energy vol 21: page 385-391

Miguel R., Espinoza R.L., Manhorn J. H., Antonio P.F (2003). Evaluation of a solar Zeolite water solar adsorption refrigerator. http://fc.uni.edu.pe/mhorn/ISES2003%20 http://fc.uni.edu.pe/mhorn/ISES2003%20(solar%20refrigeration).pdf

Nsofor E.C. (1982.) Design and construction of a air-cooled solar powered refrigeration M.Sc project Department of Mechanical Engineering. Ahmadu Bello University Zaria

Oriuwa L., (2002). Testing the stability Profile of locally synthesized Zeolite under hydrothermal condition. Final year undergraduateproject chemical Engineering Dept. A.B.U Zaria.

Polaert, I., Ledoux, A., Estel, L., Huyghe, R., and Thomas, M. (2007). Microwave Assisted Regeneration of Zeolite. International Journal of Chemical Reactor Engineering: Vol. 5: A117

Reynolds A.J. (1974): Turbulent flows in Engineering, John Wiley and sons

Siegrfried K, and Detlef B: Experiment on Solar adsorption refrigeration, using Zeolite and water. http://www.containedenergy.com/html/zeolite_cooling.html

Solar adsorption refrigerator www.needfulprovision.org/main/solarovenphp

Sumathy. K. and Zhongfu Li. (1999). A solar-powered ice-maker with the solid adsorption pair of activated carbon and methanol. International Journal of Energy Research, 23, 517-527.

Tchevner D. I: (1983) Use of natural Zeolites in solar refrigeration :ASSETS Abstracts of selected solar energy technology pp 21-23

Valan Arasu, A., Sornakumar, T., Performance.(2006), Characteristics of Parabolic Trough Solar Collector System for Hot Water Generation, The International Energy Journal, 7 2, pp. 137-145

Wang, R.Z.,.Jia J.P, Zhu Y.H., Teng Y., Wu J.Y and Cheng J.. (1997). Study on a new solid adsorption refrigeration pair: active carbon fibre-methanol. *ASME J. Solar Energy Engg*, *119*, 214-219.

Xia Z.Z, Wang R.Z. , Lu Z.S. and Wang L.W (2007). Two Heat Pipe Type High Efficient Adsorption Icemakers for Fishing Boats Open Chemical Engineering Journal, 2007, 1, 17-22

APPENDIX A

Rim Angle		Approx. Collector Efficiency	Focal Length		Approx. Receiver OD		Arc Length		Remarks
(Rad)	(Deg)	(%)	(mm)	(in)	(mm)	(in)	(mm)	(in)	
1.22	70 (Trimmed 90^o 1.57 rad)	63.7	500	19.68	22.9	0.9	1.51	59.36	90^o Rim angle focal length 1.57radian 1.678 meters Aperture
1.50	80 (Trimmed 90^o 1.57 rad)	64.3	500	19.68	22.0	0.9	1.85	73.16	90^o Rim angle focal length 1.57radian 1.678 meters Aperture
0.79	45	55.97	1207	47.52	40.6	1.6	2.06	80..94	2 Meters Aperture
1.05	60	60.6	866	34.10	35.6	1.4	2.11	82.92	2 Meters Aperture
1.22	70	62.4	714	28.11	28.7	1.13	2.15	84.77	2 Meters Aperture
1.40	80	63.8	596	23.46	26.7	1.05	2.21	87.19	2 Meters Aperture
1.57	90	64.6	500	19.68	25.4	1.00	2.30	90.38	2 Meters Aperture
1.66	95	64.9	458	18.04	25.4	1.00	2.35	92.35	2 Meters Aperture
1.75	100	65.0	420	16.52	24.1	0.95	2.40	94.64	2 Meters Aperture
1.83	105	65.1	384	15.10	24.1	0.95	2.47	97.31	2 Meters Aperture
1.92	110	65.0	350	13.78	24.1	0.95	2.55	100.46	2 Meters Aperture
2.09	120	64.8	289	11.37	24.1	0.95	2.76	108.67	2 Meters Aperture

APPENDIX B

Synthesis of Zeolite A

The synthesis and was done in a manner similar to that reported by Aderemi, B.O., 2004.and Oriuwa Lazarus Jan 2002

Molecular formula for Zeolite = $Al_2O_3.2SiO_2$

Molecular mass of Metakaolin = 102 + 2(60) = 222g

$\frac{SiO_2}{Al_2O_3}$ = 2, $\frac{Na_2O}{Al_2O_3}$ = 2.4, $\frac{H_2O}{Al_2O_3}$ = 9.6

222g of metakaolin → 102g of Al_2O_3

600g of metakaolin → $\frac{600 \times 102}{222}$ = 275.68g of AL_2O_3

Moles of Al_2O_3 → $\frac{275.68}{102}$ = 2.7moles

1mole of AL_2O_3 → 2.4moles of Na_2O
2.7moles of AL_2O_3 → 2.7 x 2.4 = 6.48moles of Na_2O

$H_2O + Na_2O$ → 2NaOH

6.48 2(6.48) = 12.96

12.96moles of NaOH = $\frac{\text{Mass}}{\text{Molar mass}}$

Mass of NaOH = 12.96 x 40 = 518.4g

1mole of AL_2O_3 → 96 moles of H_2O

2.7moles of Al_2O_3 → 2.7 x 9.6 = 259.2 moles of water

Mass of water required = 259.18 x 18 = 4.665g of water

APPENDIX C

TABLE 4.10 TGA/DTA results for kaolin

Run Date: 2-Mar-08 18:11
Program: Universal V2.6D Run Number: 339

TA Instruments Thermal Analysis -- TGA-DTA

Sample: Kaolinamber
Size: 15.9319 mg
Cell Constant: 1.0000
Operator: ATTA

Comment: No N2 flow
Exotherm: Up

Temperature	Weight	Temperature Difference
°C	%	°C/mg
0.00		
10.00		
20.00		
30.00	99.93	-0.1058
40.00	99.79	-0.1873
50.00	99.58	-0.2454
60.00	99.28	-0.2761
70.00	98.98	-0.2912
80.00	98.73	-0.3000
90.00	98.53	-0.3014
100.00	98.38	-0.2973
110.00	98.27	-0.2907
120.00	98.19	-0.2826
130.00	98.14	-0.2755
140.00	98.09	-0.2708
150.00	98.04	-0.2693
160.00	97.97	-0.2694
170.00	97.91	-0.2657
180.00	97.88	-0.2584
190.00	97.86	-0.2516
200.00	97.85	-0.2461
210.00	97.83	-0.2414
220.00	97.82	-0.2369
230.00	97.81	-0.2324
240.00	97.79	-0.2279

250.00	97.78	-0.2234
260.00	97.76	-0.2190
270.00	97.75	-0.2147
280.00	97.74	-0.2108
290.00	97.72	-0.2074
300.00	97.71	-0.2042
310.00	97.69	-0.2013
320.00	97.68	-0.1987
330.00	97.66	-0.1965
340.00	97.64	-0.1946
350.00	97.63	-0.1932
360.00	97.61	-0.1922
370.00	97.59	-0.1916
380.00	97.57	-0.1914
390.00	97.55	-0.1916
400.00	97.52	-0.1922
410.00	97.49	-0.1934
420.00	97.46	-0.1947
430.00	97.42	-0.1954
440.00	97.37	-0.1983
450.00	97.31	-0.2033
460.00	97.23	-0.2090
470.00	97.12	-0.2166
480.00	96.97	-0.2273
490.00	96.75	-0.2434
500.00	96.41	-0.2664
510.00	95.92	-0.2963
520.00	95.22	-0.3321
530.00	94.30	-0.3692
540.00	93.20	-0.3958
550.00	92.03	-0.4079
560.00	90.96	-0.3977
570.00	90.06	-0.3721
580.00	89.31	-0.3455
590.00	88.69	-0.3234
600.00	88.16	-0.3053
610.00	87.74	-0.2902
620.00	87.40	-0.2781
630.00	87.12	-0.2699
640.00	86.89	-0.2642
650.00	86.70	-0.2591
660.00	86.54	-0.2559
670.00	86.41	-0.2537
680.00	86.31	-0.2517
690.00	86.23	-0.2507
700.00	86.15	-0.2510

710.00	86.09	-0.2515
720.00	86.03	-0.2520
730.00	85.98	-0.2526
740.00	85.93	-0.2531
750.00	85.89	-0.2536
760.00	85.85	-0.2537
770.00	85.82	-0.2537
780.00	85.79	-0.2540
790.00	85.76	-0.2543
800.00	85.74	-0.2548
810.00	85.72	-0.2553
820.00	85.70	-0.2566
830.00	85.68	-0.2586
840.00	85.66	-0.2606
850.00	85.64	-0.2629
860.00	85.62	-0.2653
870.00	85.61	-0.2675
880.00	85.59	-0.2701
890.00	85.57	-0.2730
900.00	85.56	-0.2755
910.00	85.54	-0.2737
920.00	85.53	-0.2770
930.00	85.51	-0.2808
940.00	85.50	-0.2848
950.00	85.49	-0.2889
960.00	85.48	-0.2911
970.00	85.47	-0.2904
980.00	85.46	-0.2750
990.00		
1000.00		

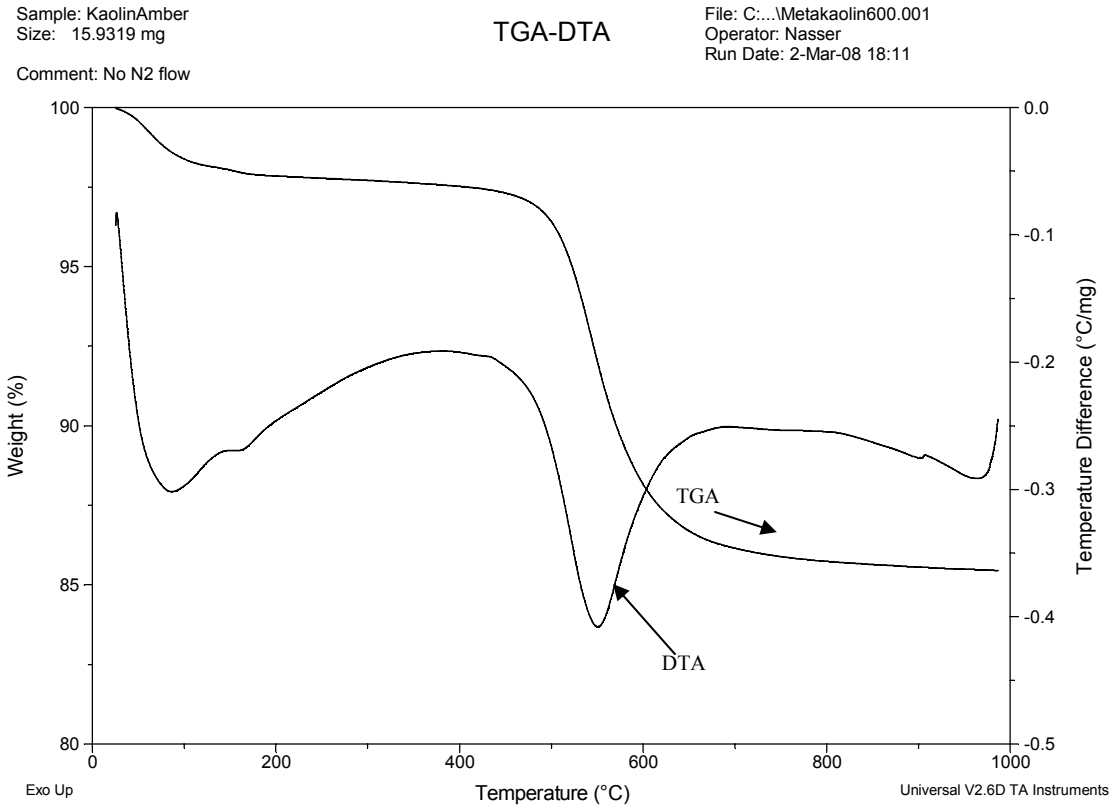


Fig 4.10 TGA/DTA graph for kaolin

TABLE 4.11 TGA/DTA results for Metakaolin

Run Date: 3-Mar-08 18:35
Program: Universal V2.6D Run Number: 341

TA Instruments Thermal Analysis -- TGA-DTA

Sample: Metakaolinamber
Size: 12.7063 mg
Cell Constant: 1.0000
Operator: Nasser

Comment: No N2 flow
Exotherm: Up

Temperature	Weight	Temperature Difference
°C	%	°C/mg
0.00		
10.00		
20.00		
30.00	99.89	-0.1497
40.00	99.69	-0.2369
50.00	99.48	-0.2726
60.00	99.36	-0.2726
70.00	99.29	-0.2730
80.00	99.23	-0.2787
90.00	99.17	-0.2850
100.00	99.12	-0.2892
110.00	99.08	-0.2920
120.00	99.03	-0.2935
130.00	99.00	-0.2940
140.00	98.96	-0.2932
150.00	98.93	-0.2914
160.00	98.90	-0.2887
170.00	98.87	-0.2854
180.00	98.84	-0.2815
190.00	98.81	-0.2771
200.00	98.78	-0.2724
210.00	98.76	-0.2677
220.00	98.73	-0.2628
230.00	98.70	-0.2579
240.00	98.68	-0.2528
250.00	98.65	-0.2479

260.00	98.62	-0.2434
270.00	98.59	-0.2394
280.00	98.56	-0.2360
290.00	98.53	-0.2334
300.00	98.50	-0.2311
310.00	98.47	-0.2292
320.00	98.44	-0.2278
330.00	98.40	-0.2268
340.00	98.37	-0.2260
350.00	98.33	-0.2255
360.00	98.29	-0.2250
370.00	98.26	-0.2249
380.00	98.22	-0.2253
390.00	98.18	-0.2254
400.00	98.15	-0.2256
410.00	98.11	-0.2263
420.00	98.07	-0.2270
430.00	98.03	-0.2263
440.00	97.99	-0.2264
450.00	97.94	-0.2291
460.00	97.90	-0.2306
470.00	97.86	-0.2320
480.00	97.82	-0.2341
490.00	97.78	-0.2363
500.00	97.75	-0.2397
510.00	97.72	-0.2435
520.00	97.69	-0.2473
530.00	97.67	-0.2492
540.00	97.65	-0.2460
550.00	97.63	-0.2455
560.00	97.61	-0.2476
570.00	97.59	-0.2504
580.00	97.58	-0.2534
590.00	97.56	-0.2564
600.00	97.55	-0.2597
610.00	97.53	-0.2633
620.00	97.52	-0.2675
630.00	97.49	-0.2717
640.00	97.47	-0.2752
650.00	97.45	-0.2778
660.00	97.43	-0.2810
670.00	97.41	-0.2852
680.00	97.40	-0.2890
690.00	97.37	-0.2931
700.00	97.35	-0.2974
710.00	97.32	-0.3016

720.00	97.29	-0.3056
730.00	97.25	-0.3094
740.00	97.20	-0.3121
750.00	97.15	-0.3139
760.00	97.11	-0.3145
770.00	97.06	-0.3144
780.00	97.02	-0.3141
790.00	96.98	-0.3132
800.00	96.95	-0.3121
810.00	96.91	-0.3110
820.00	96.88	-0.3107
830.00	96.86	-0.3113
840.00	96.83	-0.3125
850.00	96.82	-0.3144
860.00	96.80	-0.3166
870.00	96.78	-0.3189
880.00	96.77	-0.3211
890.00	96.75	-0.3238
900.00	96.74	-0.3267
910.00	96.73	-0.3302
920.00	96.72	-0.3330
930.00	96.72	-0.3350
940.00	96.71	-0.3394
950.00	96.70	-0.3446
960.00	96.70	-0.3465
970.00	96.69	-0.3413
980.00	96.69	-0.3100
990.00		
1000.00		

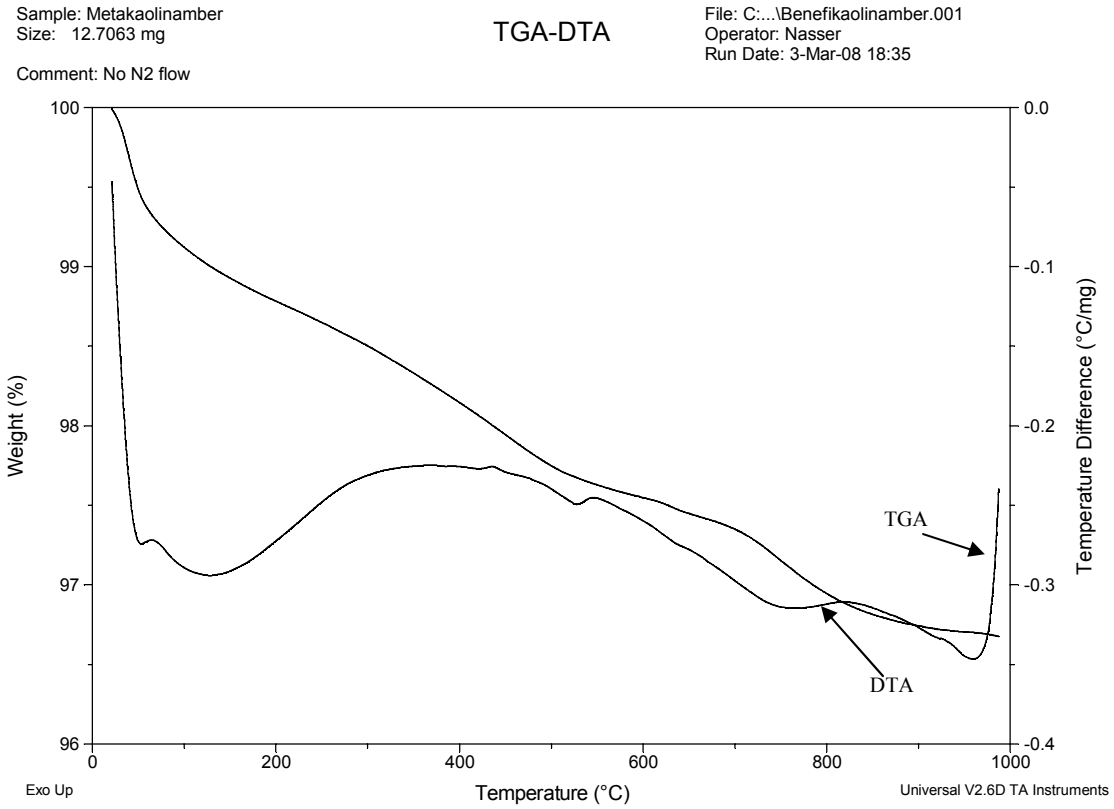


Fig 4.11 TGA/DTA graph for metakoalin

TABLE 4.12 TGA/DTA results for Zeolite

Run Date: 2-Mar-08 14:45
Program: Universal V2.6D Run Number: 338

TA Instruments Thermal Analysis -- TGA-DTA

Sample: ZeoliteAmber
Size: 11.5234 mg
Cell Constant: 1.0000
Operator: ATTA

Comment: No N2 flow
Exotherm: Up

Temperature	Weight	Temperature Difference
°C	%	°C/mg
0.00		
10.00		
20.00		
30.00	99.89	-0.1727
40.00	99.69	-0.2927
50.00	99.35	-0.3761
60.00	98.89	-0.4241
70.00	98.38	-0.4586
80.00	97.85	-0.4891
90.00	97.27	-0.5152
100.00	96.64	-0.5354
110.00	95.97	-0.5504
120.00	95.22	-0.5651
130.00	94.40	-0.5784
140.00	93.49	-0.5910
150.00	92.45	-0.6045
160.00	91.30	-0.6161
170.00	90.05	-0.6220
180.00	88.76	-0.6174
190.00	87.53	-0.5985
200.00	86.44	-0.5622
210.00	85.57	-0.5110
220.00	84.94	-0.4527
230.00	84.50	-0.3985
240.00	84.19	-0.3558
250.00	83.96	-0.3262
260.00	83.76	-0.3065

270.00	83.60	-0.2931
280.00	83.45	-0.2841
290.00	83.31	-0.2789
300.00	83.17	-0.2762
310.00	83.03	-0.2748
320.00	82.88	-0.2739
330.00	82.73	-0.2734
340.00	82.58	-0.2731
350.00	82.43	-0.2730
360.00	82.27	-0.2727
370.00	82.11	-0.2723
380.00	81.95	-0.2715
390.00	81.80	-0.2704
400.00	81.65	-0.2693
410.00	81.51	-0.2676
420.00	81.38	-0.2649
430.00	81.26	-0.2596
440.00	81.15	-0.2564
450.00	81.05	-0.2553
460.00	80.96	-0.2531
470.00	80.89	-0.2518
480.00	80.82	-0.2504
490.00	80.76	-0.2501
500.00	80.70	-0.2525
510.00	80.65	-0.2556
520.00	80.60	-0.2591
530.00	80.54	-0.2598
540.00	80.50	-0.2533
550.00	80.46	-0.2505
560.00	80.42	-0.2508
570.00	80.38	-0.2516
580.00	80.34	-0.2528
590.00	80.31	-0.2541
600.00	80.27	-0.2557
610.00	80.24	-0.2577
620.00	80.20	-0.2598
630.00	80.17	-0.2619
640.00	80.14	-0.2631
650.00	80.10	-0.2638
660.00	80.08	-0.2652
670.00	80.05	-0.2678
680.00	80.03	-0.2686
690.00	80.01	-0.2700
700.00	80.00	-0.2713
710.00	79.98	-0.2724
720.00	79.97	-0.2737

730.00	79.96	-0.2746
740.00	79.94	-0.2751
750.00	79.93	-0.2751
760.00	79.92	-0.2742
770.00	79.90	-0.2723
780.00	79.89	-0.2695
790.00	79.87	-0.2657
800.00	79.85	-0.2617
810.00	79.83	-0.2589
820.00	79.81	-0.2587
830.00	79.79	-0.2633
840.00	79.77	-0.2692
850.00	79.76	-0.2739
860.00	79.76	-0.2799
870.00	79.75	-0.2873
880.00	79.76	-0.2943
890.00	79.76	-0.3029
900.00	79.76	-0.3103
910.00	79.77	-0.3171
920.00	79.79	-0.3233
930.00	79.81	-0.3296
940.00	79.83	-0.3360
950.00	79.86	-0.3426
960.00	79.90	-0.3491
970.00	79.94	-0.3516
980.00	79.98	-0.3537
990.00		
1000.00		

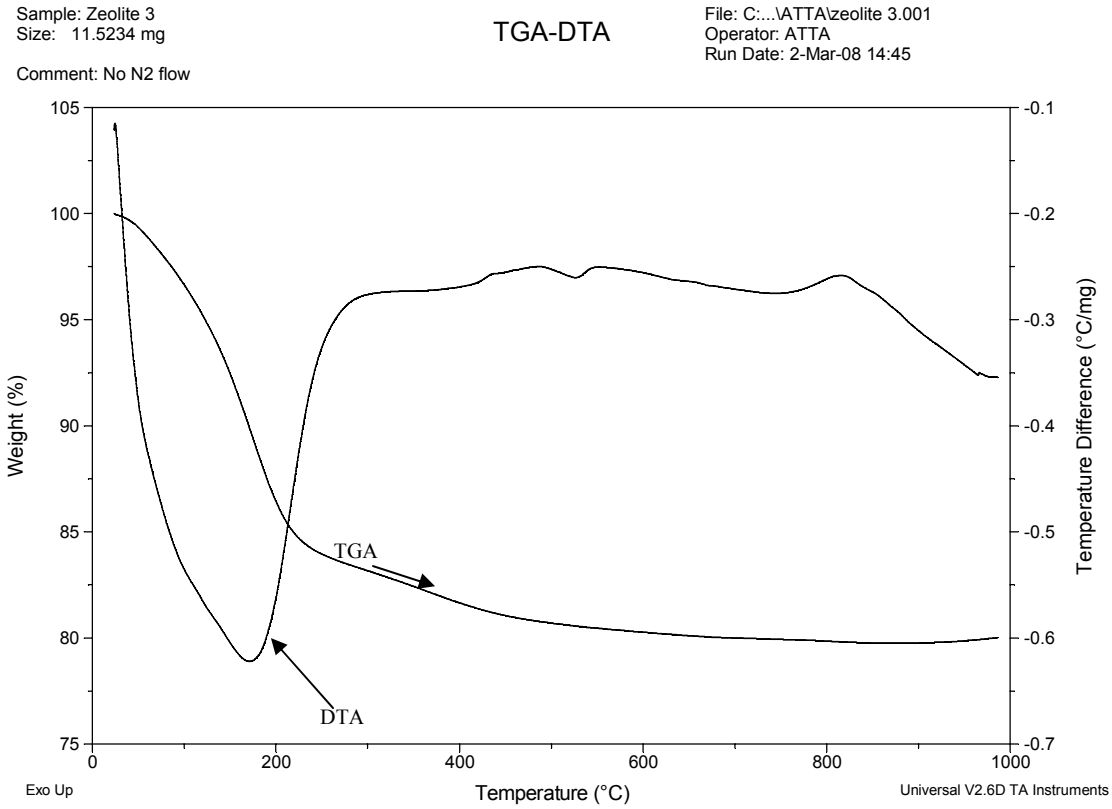


Fig 4.12. TGA/DTA graph for Zeolite A